

J. Hansen · J. Pospiech · K. Lücke

Tables for Texture Analysis of Cubic Crystals



Springer-Verlag Berlin · Heidelberg · New York

J. Hansen • J. Pospiech • K. Lücke

Tables for Texture Analysis of Cubic Crystals



Springer-Verlag
Berlin • Heidelberg • New York 1978

Dr. rer. nat. Jörn Hansen

Member of the Institute for Materials Research of the German Aero-Space Research Establishment (Institut für Werkstoff-Forschung der Deutschen Forschungs- und Versuchsanstalt für Luft- und Raumfahrt e.V.),
Köln, West-Germany.

Dr. Jan Pospiech

Member of the Institute for Metal Research of the Polish Academy of Sciences (Polska Akademia Nauk, Zakład Podstaw Metalurgii),
Kraków, Poland.

Prof. Dr. rer. nat. Kurt Lücke

Director of the Institute for Physical Metallurgy and Metal Physics at the Rhenian Westphalian Institute of Technology (Institut für Allgemeine Metallkunde und Metallphysik der Rheinisch-Westfälischen Technischen Hochschule),
Aachen, West-Germany.

ISBN 3-540-08689-7 Springer-Verlag Berlin-Heidelberg-New York

ISBN 0-387-08689-7 Springer-Verlag New York-Heidelberg-Berlin

Library of Congress Cataloging in Publication Data. Hansen, Jörn, 1940- Tables for texture analysis of cubic crystals. Bibliography: p. Includes index. 1. Texture (Crystallography) -Tables. I. Pospiech, Jan, 1936- joint author. II. Lücke, Kurt, joint author. III. Title. QD921.H33 547'.8 78-2014

This digital version has been revised by Prof. Dr. Jan Pospiech.
Included is the FORTRAN listing of the ODF program which was published in

J. Jura, J. Pospiech and H.J. Bunge: *Ein Standardsystem von Rechenprogrammen der dreidimensionalen Texturanalyse*.
Metalurgia 24 (1976) 111-176 Polska Akademia Nauk, Cracow.

Section B: The Tables have been omitted in the digital version.

© Prof. Dr. Jan Pospiech, Cracow 2016.

This work is subject to copyright. All rights reserved, whether the whole or part of the material is concerned, specifically those of translation, reprinting, re-use of illustrations, broadcasting, reproduction by photocopying machine or similar means, and storage in data banks. Under § 54 of the German Copyright Law where copies are made for other than private use, a fee is payable to the publisher, the amount of the fee to be determined by agreement with the publisher.

© Springer-Verlag, Berlin—Heidelberg 1978. Printed in Germany.

Composition and Design: Verena Boldin, Aachen; Printing and Binding: E. Hunko, Aachen.

The use of registered names, trademarks, etc. in this publication does not imply, even in the absence of a specific statement, that such names are exempt from the relevant protective laws and regulations and therefore free for general use.

P R E F A C E

Recent progress in the material sciences has led to an increasing amount of interest in the role of textures for the behaviour of materials and in the mechanisms controlling the texture formation. This development was supported by a rather powerful development taking place in the area of texture studies itself: Besides the usual, more qualitative, characterization of a texture by pole figures a fully quantitative description by a three-dimensional orientation distribution function (ODF) has been increasingly applied.

There are two sides to the problem of quantitative representation of textures. One involves the mathematical technique associated with the acquisition of an ODF, and its transforms, from the experimental data, whereas the other concerns the methods of a rational description and interpretation of an ODF.

The first side can be considered from the practical point of view as experimental-data processing which is accomplished by a computer and is sort of a continuation of the measurement itself. Much attention has been paid to this problem, particularly by Bunge, who has written up achievements in this field in this extensive monograph /1/ and in conference proceedings /2/. There is also available a rather detailed presentation of a system of subroutines written in Fortran /3/ which allows standard computations to be made without having to go into the mathematical details of the method.

The second side of the problem is the concern of the present study which contains information facilitating the analysis of an ODF obtained by calculative methods. The ODF defines the frequency of occurrence of a given orientation in a sample and is presented in a three-dimensional space formed by the three parameters describing an orientation, usually by the three Euler angles. For the purpose of approximate description and interpretation of the ODF, "ideal orientations" or "components" are often identified and crystallographic relationships between the components determined (e. g. twin relationships). This allows simple comparison to mathematical or physical models.

The present "Tables" give the most important notions and auxiliary data used in texture analysis on the basis of ODF's and of pole figures. The largest part of this work is tabulated data presenting numerical relationships between Miller indices, Euler angles and pole figure positions. Such data is very important and helpful in almost all texture investigations. The lack of a generally accessible collection of such data has frequently made it necessary to calculate appropriate tabular values separately as appendices of publications.

The tables are limited to cubic crystal symmetry. They are further limited to orientations characterized by Miller indices with $0 \leq h, k, l, u, v, w \leq 15$ or ≤ 12 , respectively. But even then nearly 15000 different orientations had to be considered. The authors regret that the use of the tables is not as simple as e.g. the use of logarithm tables. They hope, however, that — with the aid of the explanations before each table — they will quickly become a useful tool for researchers in the area of texture analysis.

Especially emphasized shall also be the first part of this book. In a rather complete but also easily accessible form it contains a detailed review of the different ways of representing orientation distributions and orientation relationships including the most important mathematical derivations in this field. Particularly the symmetry relations in the Euler angle space — hitherto a little known although rather important area — have been thoroughly discussed. In order to achieve an optimum understanding also original contributions not published elsewhere are included into this review.

The authors are deeply indebted to Dip.-Ing. K.H. Virnich for his continuous assistance and for numerous valuable discussions and contributions. They acknowledge the understanding shown for this work by Prof. W. Bunk, Köln, and Prof. Truskowski, Krakow. They like to express their gratitude to Mrs. V. Boldin and to the staff of the computer center of the RWTH Aachen and of the DFVLR, Köln, for valuable aid in calculating and printing the tables.

CONTENTS

	side
A Review of the Representation of Orientations and Orientation Distributions	5
1. Introduction	5
2. Representation of an Orientation	6
2.1 Definition of Orientation	6
2.2 Description of an Orientation by the Miller Indices (HKL) [UVW]	7
2.3 Description of an Orientation by the Euler Angles $\varphi_1 \phi \varphi_2$	8
2.4 Description of an Orientation by the Euler Angles $\psi \theta \phi$	9
2.5 Description of an Orientation by Rotational Coordinates \vec{v}, ω	11
2.6 Description of an Orientation by Pole Figures	12
2.7 Description of an Orientation by Inverse Pole Figures	14
2.8 Relationships Between the Different Types of Orientation Parameters	14
3. The Orientation Space	16
3.1 Examples for Various Types of Orientation Spaces	16
3.2 Symmetrically Equivalent Orientations	18
3.3 Symmetries of the Euler Angle Space due to Identical Equivalencies	21
3.4 Symmetries of the Euler Angle Space Induced by the Cubic Crystal Symmetry	22
3.5 Symmetries of the Euler Angle Space in the Case of Orthorhombic Sample Symmetry	24
3.6 Symmetries of the Euler Angle Space in the Case of Lower Sample Symmetry	28
4. Representation of Orientation Distributions in the Euler Angle Space	29
4.1 The Orientation Distribution Function (ODF)	29
4.2 Distortion of the Euler Angle Space Near $\phi = 0$; Texture Components	30
4.3 Meaning of Special Lines and Planes in the Euler Angle Space	32
4.4 The Multiplicity of Orientations	33
4.5 The ODF in Equivalent Regions	36
4.6 Orientation Transformations and Orientation Relationships	36
Appendix	39
References	40

B The Tables

Table I:	The General Miller-Indices {HKL} <UVW> for H,K,L,U,V,W ≤ 15
Table II:	From the {001}-Pole Figure to Miller Indices
Table III:	From {011} Pole Figure to Miller Indices
Table IV:	From {111} Pole Figure to Miller Indices
Table V:	From Miller Indices into Euler Angles
Table VI:	From Euler Angles into Miller Indices
Table VII:	Angles between Sample and Crystal Axes

A. REVIEW OF THE REPRESENTATION OF ORIENTATIONS AND ORIENTATION DISTRIBUTIONS

1. INTRODUCTION

One of the most important quantities describing the internal structure of a polycrystalline material is the distribution of the orientations of its crystallites. This orientation distribution is commonly denoted as texture. The accepted practice is to speak of a texture when the orientation distribution is not a random one.

Texture analysis is based on a simple geometrical model in which the polycrystalline aggregate is represented by rectangular right-handed reference frames associated with the sample and with the crystallographic lattice of the crystallites. The axes of the sample reference system are chosen mostly in accordance with the external shape of the sample or, if its orientation distribution is symmetrical, in accordance with this symmetry. E.g. in the case of a rolled sheet, usually the rolling direction (RD), the transverse direction (TD) and the normal direction (ND) are used. The axes of the crystal reference systems are chosen parallel to (mostly low indexed) crystallographic directions, e.g. in the case of cubic symmetry parallel to the three edges of the cubic cell [100], [010] and [001], respectively. These frames are thought to be brought to a common origin at which also the center of point symmetry is located.

The fundamental notion when describing textures is the orientation of a crystallite. It is defined as the position of the reference frame of the crystallite relative to that of the sample, and thus can be expressed by the rotation of one frame into the other. Thus the notions and relationships used for describing textures are based on the properties of rotations and can be established by employing vectorial and matrix calculus. Since for the determination of a rotation 3 parameters are needed, an orientation can be represented by a point in a 3-dimensional "orientation space" formed by the 3 orientation parameters as coordinates. In quantitative texture analysis mostly the 3 Euler angles φ_1 , ϕ , φ_2 are chosen as orientation parameters.

Another, rather illustrative way of representing an orientation is to consider a unit sphere fixed with respect to the sample frame, and to indicate on its surface the directions normal to a set of symmetrically equivalent low-indexed crystallographic planes ("poles"). The common practice is to consider the stereographic projection of this unit sphere ("pole figure") and to describe the positions of the poles by means of the spherical coordinates α , β . Frequently employed in analyzing and interpreting textures is also a description of orientations by assigning crystallographic indices (HKL) [UVW] to a certain plane of the sample and to a certain direction within this plane. E.g. in the case of a rolled sheet, (HKL) [UVW] commonly denotes the rolling plane and the rolling direction.

A texture is quantitatively described by its orientation distribution function ("ODF"). This is a density function in the three-dimensional orientation space and represents the frequency of a certain orientation as function of the 3 orientation parameters. It is obtained by numerical techniques from experimental data, which usually are pole figures, i.e. two-dimensional distribution functions of the poles of specific lattice planes. The reason for choosing this type of data is that the pole of a reflecting plane (in contrast to the angle of rotation around this pole) can be obtained rather easily by simple Debye-Scherrer X-ray technique. In practice, often the pole figures themselves (i.e. without calculating an ODF) are used to characterize a texture. They do not allow a complete recognition of the orientation distribution, but give some information about its main features, e.g. allow the identification of the orientations of the maxima of the ODF.

The following derivations are limited to cubic crystals. Furthermore, the sample geometry is mostly considered to be orthorhombic. In order to have something specific in mind, the samples will be then referred to as rolled sheets. To a certain extent, however, also monoclinic samples (e.g. sheets after uni-directional rolling) or triclinic samples (e.g. rolled single crystals) are considered. Fiber textures are not especially discussed since they are thoroughly described in /1/ and can be presented unequivocally and mostly more simply by inverse pole figures.

2. REPRESENTATION OF AN ORIENTATION

2.1 Definition of Orientation

In all what follows, the base vectors $\vec{s}_1, \vec{s}_2, \vec{s}_3$ of the reference frame S associated with the sample are chosen parallel to RD, TD and ND and the base vectors $\vec{c}_1, \vec{c}_2, \vec{c}_3$ of the frame C associated with a crystal lattice are chosen parallel to the crystallographic directions [100], [010] and [001]. The crystallite orientation is defined as the rotation which transforms the sample reference frame S into that of the crystallite C.

The base vectors of the reference frames are related through the linear relationships

$$\begin{aligned}\vec{c}_1 &= g_{11}\vec{s}_1 + g_{12}\vec{s}_2 + g_{13}\vec{s}_3 \\ \vec{c}_2 &= g_{21}\vec{s}_1 + g_{22}\vec{s}_2 + g_{23}\vec{s}_3 \\ \vec{c}_3 &= g_{31}\vec{s}_1 + g_{32}\vec{s}_2 + g_{33}\vec{s}_3\end{aligned}\tag{1}$$

In matrix notation the transformation (1) has the form

$$\begin{pmatrix} \vec{c}_1 \\ \vec{c}_2 \\ \vec{c}_3 \end{pmatrix} = g \begin{pmatrix} \vec{s}_1 \\ \vec{s}_2 \\ \vec{s}_3 \end{pmatrix} \quad \text{with } g = \begin{pmatrix} g_{11} & g_{12} & g_{13} \\ g_{21} & g_{22} & g_{23} \\ g_{31} & g_{32} & g_{33} \end{pmatrix}\tag{2}$$

or abbreviated $\{C\} = g \cdot \{S\}$. The relationship (1) and thus the matrix g describe the rotation of the frame S into frame C. Hence, according to the above definition of orientation, defines the orientation in matrix representation.

Since the 3 vectors \vec{s}_i as well as, the 3 vectors \vec{c}_i are orthogonal to each other and since, in addition, the \vec{s}_i, \vec{c}_i are supposed to be unity vectors, one has for the scalar products

$$\vec{s}_i \cdot \vec{s}_j \text{ or } \vec{c}_i \cdot \vec{c}_j = \delta_{ij} \equiv \begin{cases} 1 & \text{for } i = j \\ 0 & \text{for } i \neq j \end{cases}\tag{3}$$

With this, one obtains for the scalar products

$$\vec{c}_i \cdot \vec{s}_k = g_{ik}.\tag{4}$$

The matrix elements g_{ik} are the cosines of the angles between the base vectors \vec{c}_i and \vec{s}_k . The elements in the rows g_{ik} ($k = 1, 2, 3$) are the direction cosines of the \vec{c}_i vectors in the S system, whereas the elements in the columns g_{ik} ($i = 1, 2, 3$) are the direction cosines of the \vec{s}_i vectors in the C system.

The orthogonality of the frames expressed by Eq. (3) results in six independent conditions for elements g_{ik} . They can be written in the form

$$\sum_{k=1}^3 g_{ik} g_{jk} = \delta_{ij}\tag{5}$$

and are obtained from Eqs. (1) and (3) by taking the appropriate scalar products $\vec{c}_i \cdot \vec{c}_j$. The left-hand side of this equation represents the matrix element of the product of the matrix g and the transposed matrix g^T (which is defined by $g_{mn}^T = g_{nm}$):

$$(g \cdot g^T)_{ij} = \sum_{k=1}^3 g_{ik} g_{kj}^T = \sum_{k=1}^3 g_{ik} g_{jk}.\tag{6}$$

The right hand side represents the unity matrix E so that Eq. (5) can be written as

$$g \cdot g^T = E = \begin{pmatrix} 1 & 0 & 0 \\ 0 & 1 & 0 \\ 0 & 0 & 1 \end{pmatrix} \quad (7)$$

Since the inverse matrix g^{-1} is defined by the equation $g \cdot g^{-1} = E$, the orthogonality conditions are identical with statement that here the inverse matrix g^{-1} (which describes the transformation $\{S\} = g^{-1}\{C\}$) is equal to the transposed matrix g^T .

The coordinates (x_s, y_s, z_s) and (x_c, y_c, z_c) of any vector \vec{R} in the two reference frames S and C are transformed by the same matrices g and g^{-1} as the base vectors. With

$$\vec{R} = x_c \vec{c}_1 + y_c \vec{c}_2 + z_c \vec{c}_3 = x_s \vec{s}_1 + y_s \vec{s}_2 + z_s \vec{s}_3 \quad (8)$$

one obtains by scalar multiplication in succession by $\vec{c}_1, \vec{c}_2, \vec{c}_3$ and considering (4):

$$\begin{pmatrix} x_c \\ y_c \\ z_c \end{pmatrix} = g \begin{pmatrix} x_s \\ y_s \\ z_s \end{pmatrix}; \quad \begin{pmatrix} x_s \\ y_s \\ z_s \end{pmatrix} = g^{-1} \begin{pmatrix} x_c \\ y_c \\ z_c \end{pmatrix} \quad (9)$$

Because of the six orthogonality conditions (5) between the nine matrix elements g_{ik} , the number of independent angles defining a rotation g becomes reduced from nine to three. Hence, the description of an orientation requires only 3 angles which are called orientation parameters. They may be chosen in different ways some of them will now be discussed.

2.2. Description of an Orientation by the Miller Indices (HKL) [UVW]

A method rather frequently used for describing an orientation is to indicate rolling plane and rolling direction by the Miller indices (HKL) [UVW]. They have the advantage of directly giving an insight into the crystallographic nature of the orientation.

The indices (HKL) are assigned to the normal direction \vec{s}_3 of the sheet plane and [UVW] to the rolling direction \vec{s}_1 . They define the direction cosines of the \vec{s}_3 and \vec{s}_1 vectors in the crystallite system C according to

$$\vec{s}_3 = \frac{H}{M} \vec{c}_1 + \frac{K}{M} \vec{c}_2 + \frac{L}{M} \vec{c}_3 \quad (10)$$

$$\text{and } \vec{s}_1 = \frac{U}{N} \vec{c}_1 + \frac{V}{N} \vec{c}_2 + \frac{W}{N} \vec{c}_3 \quad (11)$$

where $M = \sqrt{H^2 + K^2 + L^2}$ and $N = \sqrt{U^2 + V^2 + W^2}$.

The vector \vec{s}_2 in TD follows from these equations according to $\vec{s}_2 = (\vec{s}_3 \times \vec{s}_1)$ or

$$\vec{s}_2 = \frac{KW - LV}{MN} \vec{c}_1 + \frac{LU - HW}{MN} \vec{c}_2 + \frac{HV - KU}{MN} \vec{c}_3 \quad (12)$$

i.e. the indices [QRS] of TD are given by

$$Q = KW - LV, \quad R = LU - HW, \quad S = HV - KU.$$

Scalar multiplication of Eqs. (10), (11) and (12) by \vec{c}_1 , \vec{c}_2 and \vec{c}_3 and consideration of (4) yields the matrix of rotations defined by the indices (HKL) [UVW]

$$g((HKL) [UVW]) = \begin{pmatrix} \frac{U}{N} & \frac{KW - LV}{MN} & \frac{H}{M} \\ \frac{V}{N} & \frac{LU - HW}{MN} & \frac{K}{M} \\ \frac{W}{N} & \frac{HV - KU}{MN} & \frac{L}{M} \end{pmatrix} \quad (13)$$

The introduction of the Miller indices reduces the number of nine quantities q_{ik} for the description of an orientation to six and, at the same time, reduces the number of the six orthogonality conditions between the g_{ik} (Eq. (5)) to the following three relationships between the H, K, L, U, V, W:

$$\begin{aligned} (H/M)^2 + (K/M)^2 + (L/M)^2 &= 1 \\ (U/N)^2 + (V/N)^2 + (W/N)^2 &= 1 \\ HU + KV + LW &= 0. \end{aligned} \quad (14)$$

2.3 Description of an Orientation by the Euler Angles φ_1 ϕ φ_2

For the purpose of quantitative texture analysis the orientations are mostly described by the three Euler angles φ_1 , ϕ , φ_2 which lead to a simpler mathematical formalism than the other orientation parameters being in use. Using Euler angles, the transformation of the sample frame S into the crystallite frame C occurs by a set of three consecutive rotations (Fig. 1):

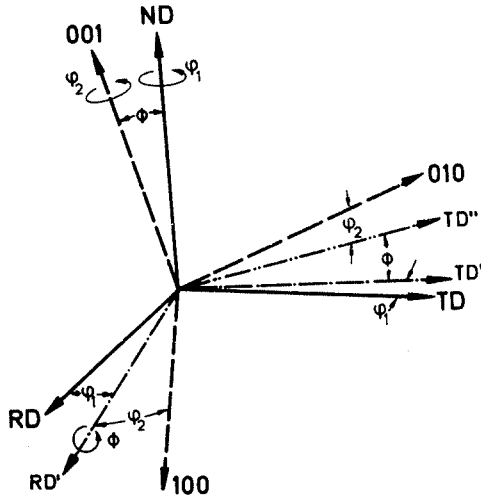


Fig. 1:
Definition of the Euler angles φ_1 , ϕ , φ_2 .

1. A first rotation φ_1 around the normal direction ND transforming the transverse direction TD and the rolling direction RD into the new directions TD' and RD', respectively. φ_1 has to have such a value that RD' will be perpendicular to the plane formed by ND and [001].
2. A second rotation ϕ around the new direction RD' with ϕ having such a value that ND is transformed into [001] (= ND') (and TD' into TD'').
3. A third rotation φ_2 around [001] (= ND') with φ_2 having such a value that RD' is transformed into [100] (and TD'' into [010]).

Scalar multiplication of Eqs. (10), (11) and (12) by \vec{c}_1 , \vec{c}_2 and \vec{c}_3 and consideration of (4) yields the matrix of rotations defined by the indices (HKL) [UVW]

$$g((HKL) [UVW]) = \begin{pmatrix} \frac{U}{N} & \frac{KW - LV}{MN} & \frac{H}{M} \\ \frac{V}{N} & \frac{LU - HW}{MN} & \frac{K}{M} \\ \frac{W}{N} & \frac{HV - KU}{MN} & \frac{L}{M} \end{pmatrix} \quad (13)$$

The introduction of the Miller indices reduces the number of nine quantities q_{ik} for the description of an orientation to six and, at the same time, reduces the number of the six orthogonality conditions between the g_{ik} (Eq. (5)) to the following three relationships between the H, K, L, U, V, W:

$$\begin{aligned} (H/M)^2 + (K/M)^2 + (L/M)^2 &= 1 \\ (U/N)^2 + (V/N)^2 + (W/N)^2 &= 1 \\ HU + KV + LW &= 0. \end{aligned} \quad (14)$$

2.3 Description of an Orientation by the Euler Angles φ_1 ϕ φ_2

For the purpose of quantitative texture analysis the orientations are mostly described by the three Euler angles φ_1 , ϕ , φ_2 which lead to a simpler mathematical formalism than the other orientation parameters being in use. Using Euler angles, the transformation of the sample frame S into the crystallite frame C occurs by a set of three consecutive rotations (Fig. 1):

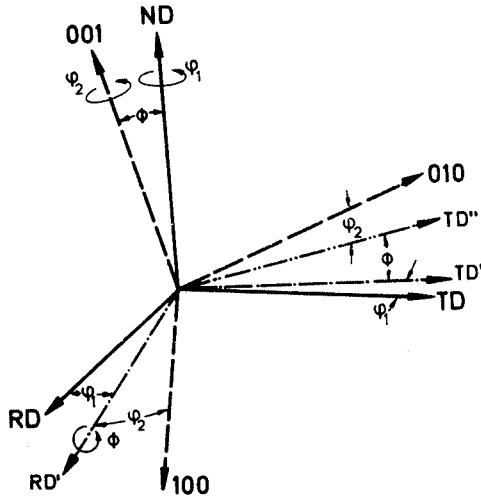


Fig. 1:
Definition of the Euler angles φ_1 , ϕ , φ_2 .

1. A first rotation φ_1 around the normal direction ND transforming the transverse direction TD and the rolling direction RD into the new directions TD' and RD', respectively. φ_1 has to have such a value that RD' will be perpendicular to the plane formed by ND and [001].
2. A second rotation ϕ around the new direction RD' with ϕ having such a value that ND is transformed into [001] (= ND') (and TD' into TD'').
3. A third rotation φ_2 around [001] (= ND') with φ_2 having such a value that RD' is transformed into [100] (and TD'' into [010]).

These 3 rotations can be expressed mathematically in the following way:

1. Rotation about \vec{s}_3 by the angle φ_1 ($\vec{s}_3 = \vec{s}_3, \vec{s}_2 \rightarrow \vec{s}_2', \vec{s}_1 \rightarrow \vec{s}_1'$) which corresponds to the transformation

$$\{S'\} = g(\varphi_1)\{S\} \quad (15)$$

$$\text{with the rotation matrix } g(\varphi_1) = \begin{pmatrix} \cos \varphi_1 & \sin \varphi_1 & 0 \\ -\sin \varphi_1 & \cos \varphi_1 & 0 \\ 0 & 0 & 1 \end{pmatrix}$$

2. about \vec{s}_1' by the angle ϕ ($\vec{s}_3' \rightarrow \vec{s}_3'', \vec{s}_2' \rightarrow \vec{s}_2'', \vec{s}_1' = \vec{s}_1''$) i.e.

$$\{S''\} = g(\phi) \cdot \{S'\} \quad (16)$$

where

$$g(\phi) = \begin{pmatrix} 1 & 0 & 0 \\ 0 & \cos \phi & \sin \phi \\ 0 & -\sin \phi & \cos \phi \end{pmatrix}$$

3. about \vec{s}_3'' by the angle φ_2 ($\vec{s}_3'' = \vec{c}_3, \vec{s}_2'' \rightarrow \vec{c}_2, \vec{s}_1'' \rightarrow \vec{c}_1$)

$$\text{i.e. } \{C\} = g(\varphi_2) \{S''\} \quad (17)$$

where

$$g(\varphi_2) = \begin{pmatrix} \cos \varphi_2 & \sin \varphi_2 & 0 \\ -\sin \varphi_2 & \cos \varphi_2 & 0 \\ 0 & 0 & 1 \end{pmatrix}$$

Successive elimination $\{S'\}$ and $\{S''\}$ from formulae (15), (16) and (17) gives the rotation matrix defined by Euler angles,

$$\{C\} = g(\varphi_2) \cdot g(\phi) \cdot g(\varphi_1) \{S\} = g(\varphi_1 \phi \varphi_2) \{S\} \quad (18)$$

which has the form:

$$g(\varphi_1 \phi \varphi_2) = \begin{pmatrix} \cos \varphi_1 \cos \varphi_2 - \sin \varphi_1 \sin \varphi_2 \cos \phi & \sin \varphi_1 \cos \varphi_2 + \cos \varphi_1 \sin \varphi_2 \cos \phi & \sin \varphi_2 \sin \phi \\ -\cos \varphi_1 \sin \varphi_2 - \sin \varphi_1 \cos \varphi_2 \cos \phi & -\sin \varphi_1 \sin \varphi_2 + \cos \varphi_1 \cos \varphi_2 \cos \phi & \cos \varphi_2 \sin \phi \\ \sin \varphi_1 \sin \phi & -\cos \varphi_1 \sin \phi & \cos \phi \end{pmatrix} \quad (19)$$

This matrix does not change if integer multiples of $\pm 2\pi$ are added to the angles $\varphi_1, \phi, \varphi_2$ or when this set of angles is replaced by

$$\varphi_1^e = \pi + \varphi_1, \quad \phi^e = -\phi, \quad \varphi_2^e = \pi + \varphi_2. \quad (20)$$

All orientations resulting from this transformations are called identically equivalent (c.f. Sec. 3.3).

2.4 Description of an Orientation by the Euler Angles $\psi \theta \phi$

In the literature also somewhat differently defined Euler angles are encountered /4/ which are denoted ψ, θ, ϕ . Their definition differs from that given above in that the second rotation (by the angle θ) takes place about the \vec{s}_2 -axis instead of about the \vec{s}_1 -axis (Fig. 2).

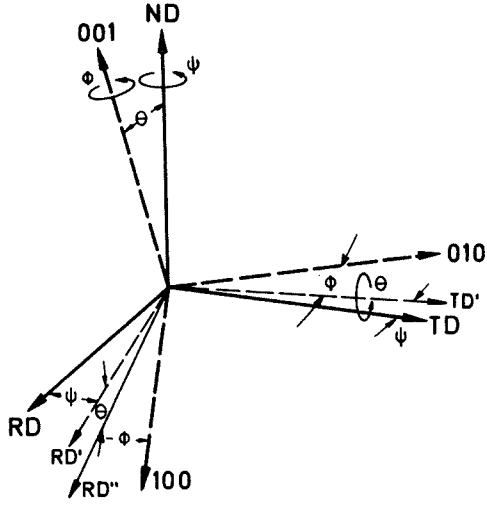


Fig. 2:
Definition of the Euler angles ψ, θ, ϕ .

The $g(\theta)$ matrix in Eq. (16) then assumes a different form,

$$g(\theta) = \begin{pmatrix} \cos \theta & 0 & -\sin \theta \\ 0 & 1 & 0 \\ \sin \theta & 0 & \cos \theta \end{pmatrix} \quad (21)$$

After the change of notation for the angles in matrices $g(\varphi_1)$ and $g(\varphi_2)$, and considering (18), we get

$$g(\phi) \cdot g(\theta) \cdot g(\psi) = g(\psi, \theta, \phi) \quad (22)$$

where

$$g(\psi, \theta, \phi) = \begin{pmatrix} \cos \phi \cos \theta \cos \psi - \sin \phi \sin \psi & \cos \phi \cos \theta \cos \psi + \sin \phi \cos \psi & -\cos \phi \sin \theta \\ -\sin \phi \cos \theta \cos \psi - \cos \phi \sin \psi & -\sin \phi \cos \theta \sin \psi + \cos \phi \cos \psi & \sin \phi \sin \theta \\ \sin \theta \cos \psi & \sin \theta \sin \psi & \cos \phi \end{pmatrix} \quad (23)$$

There exist the following general relationships between the two types of Euler angles.

$$\varphi_1 = \psi + \frac{\pi}{2}; \quad \phi = \theta; \quad \varphi_2 = \phi - \frac{\pi}{2}. \quad (24)$$

If one additionally considers cubic crystal symmetry and orthorhombic sample symmetry (Sec. 3.4) one obtains

$$\varphi_1 = \frac{\pi}{2} - \psi; \quad \phi = \theta; \quad \varphi_2 = \frac{\pi}{2} - \phi. \quad (25)$$

In Fig. 3 these relationships are illustrated in a section $\psi, \theta = \text{constant}$. One recognizes that these two sets of parameters can be transformed into each other by a two-fold axis parallel to ϕ and θ , respectively.

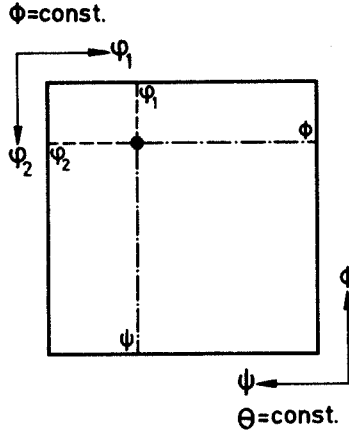


Fig. 3:
Relationships between the angles φ_1 , ϕ , φ_2 and ψ , θ , ϕ .

2.5 Description of an Orientation by Rotational Coordinates \vec{v} , ω

The rotational coordinates characterize an orientation by a single axis and angle of a rotation which transforms the S frame into C frame (Fig. 4). These coordinates have the advantage of being easy to visualize, much easier than e.g. the Euler-coordinates which describe a set of three consecutive rotations. The derivations of the expressions given in the following section can be found in /5/ and /6/.

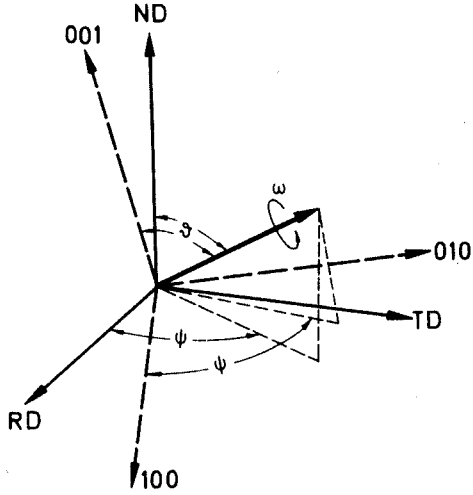


Fig. 4:
Definition of the rotational coordinates (axis of rotation $\vec{v} = \{\vartheta, \psi\}$, angle of rotation ω).

In the following ϑ and ψ shall denote the spherical coordinates of the unit vector \vec{v} which indicates the axis of rotation and ω shall be the angle of rotation around \vec{v} . As can be recognized from Fig. 4, the values of the spherical coordinates ϑ and ψ are equal in both reference frames S and C. That means that the direction cosines v_x , v_y , v_z of the rotation axis \vec{v} satisfy the condition

$$\vec{v} = v_x \vec{s}_1 + v_y \vec{s}_2 + v_z \vec{s}_3 = v_x \vec{c}_1 + v_y \vec{c}_2 + v_z \vec{c}_3$$

by scalar multiplication in succession by \vec{s}_1 , \vec{s}_2 or \vec{s}_3 (c.f. Eq. (4)) one obtains

$$\begin{pmatrix} v_x \\ v_y \\ v_z \end{pmatrix} = g \cdot \begin{pmatrix} v_x \\ v_y \\ v_z \end{pmatrix} \quad (26)$$

i.e. the rotation axes \vec{v} are eigen-vectors of the matrix g . The angle of rotation ω and the direction cosines of the rotation axis \vec{v} can be calculated from the elements g_{ik} of the matrix g in the following way

$$\begin{aligned} g_{11} + g_{22} + g_{33} &= 1 + 2 \cos \omega \\ \frac{1}{2} (g_{23} - g_{32}) &= v_x \sin \omega \\ \frac{1}{2} (g_{31} - g_{13}) &= v_y \sin \omega \\ \frac{1}{2} (g_{12} - g_{21}) &= v_z \sin \omega \end{aligned} \quad (27)$$

The matrix expressed in terms of parameters ϑ , ψ , ω in the transformation

$$\{C\} = g(\vartheta, \psi, \omega) \cdot \{S\} = g(\vec{v}, \omega) \cdot \{S\} \quad (28)$$

possesses the following form:

$$g(\vec{v}, \omega) = \begin{pmatrix} (1 - v_x^2) \cos \omega + v_x^2 & v_x v_y (1 - \cos \omega) + v_z \sin \omega & v_x v_z (1 - \cos \omega) + v_y \sin \omega \\ v_x v_y (1 - \cos \omega) - v_z \sin \omega & (1 - v_y^2) \cos \omega + v_y^2 & v_y v_z (1 - \cos \omega) + v_x \sin \omega \\ v_x v_y (1 - \cos \omega) + v_z \sin \omega & v_y v_z (1 - \cos \omega) - v_x \sin \omega & (1 - v_z^2) \cos \omega + v_z^2 \end{pmatrix} \quad (29)$$

where

$$v_x = \cos \psi \sin \vartheta; \quad v_y = \sin \psi \sin \vartheta; \quad v_z = \cos \vartheta.$$

The matrix (29) does not change if integer multiples of $\pm 2\pi$ are added to the angles ϑ , ψ , ω or when this set of angles is replaced by

$$\begin{aligned} \vartheta' &= -\vartheta & \vartheta' &= \pi - \vartheta \\ \psi' &= \pi + \psi & \text{or by} & \psi' = \pi + \psi \\ \omega' &= \omega & \omega' &= -\omega, \end{aligned} \quad (30)$$

respectively.

2.6 Description of an Orientation by Pole Figures

In a pole figure an orientation is defined by the positions of the poles ($X_i Y_i Z_i$) of the symmetrically equivalent lattice planes $\{XYZ\}$. These positions can be visualized as the intersection points of the normals to these planes with the surface of a unit sphere which is bound to the S-frame (sample). It can graphically be represented on the stereographic projection of the unit sphere („pole figure”) and numerically be described by the spherical coordinates α_i , β_i . Fig. 5 a gives an example for the $\{001\}$ poles of an arbitrary oriented crystal. Fig. 5 b indicates the projection of the intersection points into the equatorial plane and Fig. 5 c shows for one pole the angles α_i , β_i within this plane.

If R_i is the unit vector of the pole ($X_i Y_i Z_i$) then, according to Eq. (8), it has the following components in the sample's frame S (i.e. in the pole figure) and in the crystallite's frame C (i.f. also Fig. 5):

$$\begin{aligned} \vec{R}_i &= (\sin \alpha_i \cos \beta_i) \vec{s}_1 + (\sin \alpha_i \sin \beta_i) \vec{s}_2 + (\cos \alpha_i) \vec{s}_3 \\ &= \frac{1}{P} (X_i \vec{c}_1 + Y_i \vec{c}_2 + Z_i \vec{c}_3). \end{aligned} \quad (31)$$

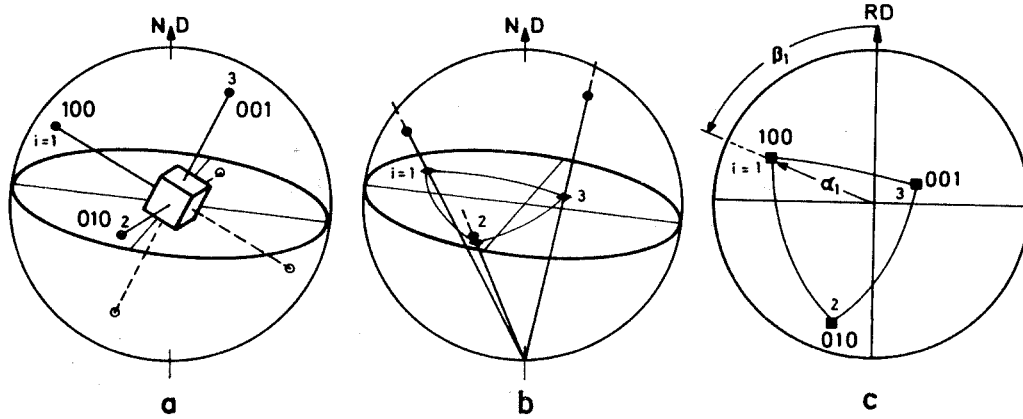


Fig. 5:
Presentation of a $\{100\}$ -pole figure. a) Position of a crystal in the center of the orientation sphere; b) Projection of the cube half axes on the equatorial plane, c) $\{100\}$ -pole figure and definition of the spherical coordinates α_i, β_i of the pole i .

Here the quantity $P = \sqrt{X_1^2 + Y_1^2 + Z_1^2}$ has the same value for all symmetrically equivalent poles $(X_i Y_i Z_i)$, i.e. it is independent of i . Scalar multiplications of Eq. (31) in succession by the three vectors \vec{s}_i and taking into consideration Eq. (4) yields the following transformation:

$$\begin{pmatrix} \sin \alpha_i \cos \beta_i \\ \sin \alpha_i \sin \beta_i \\ \cos \alpha_i \end{pmatrix} = \frac{1}{P} \begin{pmatrix} g_{11} & g_{21} & g_{31} \\ g_{12} & g_{22} & g_{32} \\ g_{13} & g_{23} & g_{33} \end{pmatrix} \begin{pmatrix} X_i \\ Y_i \\ Z_i \end{pmatrix} \quad (32)$$

It is to be recognized that here matrix $g^T = g^{-1}$ appears.

This equation allows the matrix elements g_{ik} to be determined from the poles $(X_i Y_i Z_i)$ given by the angles α_i, β_i . If, for example, for the three $\{001\}$ -poles

$$\begin{aligned} X_1 &= 1, \quad Y_1 = 0, \quad Z_1 = 0 \text{ the coordinates } \alpha_1, \beta_1 \\ X_2 &= 0, \quad Y_2 = 1, \quad Z_2 = 0 \text{ the coordinates } \alpha_1, \beta_2 \\ X_3 &= 0, \quad Y_3 = 0, \quad Z_3 = 1 \text{ the coordinates } \alpha_3, \beta_3 \end{aligned}$$

have been found, Eq. (32) yields the following nine equations for the g_{ik} :

$$g_{11} = \sin \alpha_i \cos \beta_i; \quad g_{12} = \sin \alpha_i \sin \beta_i; \quad g_{13} = \cos \alpha_i. \quad (33)$$

Because of the six orthogonality conditions between the nine g_{ik} , it would suffice to consider only 3 angles (two α_i and one β_i or vice versa), i.e. two poles only. In practice, however, it is better to use all poles and to apply the orthogonality conditions as a control. Then, by equating the nine calculated g_{ik} with the elements of the matrix Eq. (19) (or Eqs. (23), (29) or (13)), the three Euler angles (or any other three orientation parameters) can be derived. Also here not all nine equations have to be solved, three independent equations would suffice. However, because of the multivalency of the trigonometric functions, sometimes five equations are necessary in order to fix also the signs of the angles*.

Conversely, if the orientation g is given, the positions α_i, β_i of the poles $(X_i Y_i Z_i)$ in the pole figure can be calculated from the g_{ik} . For example, the position α_i, β_i of the pole (111) (i.e. $X_1 = Y_1 = Z_1 = 1$) of the orientation (101) $[\bar{1}\bar{2}1]$ are found from Eqs. (13) and (32):

* Often it is faster and more practical to derive the poles $(X_i Y_i Z_i)$ in a graphical way. Such a method for obtaining the poles from the Euler angles is described in Appendix I.

$$\begin{pmatrix} \sin \alpha_1 \cos \beta_1 \\ \sin \alpha_1 \sin \beta_1 \\ \cos \alpha_1 \end{pmatrix} = \frac{1}{\sqrt{3}} \begin{pmatrix} -\frac{1}{\sqrt{6}} & -\frac{2}{\sqrt{6}} & \frac{1}{\sqrt{6}} \\ \frac{1}{\sqrt{3}} & -\frac{1}{\sqrt{3}} & -\frac{1}{\sqrt{3}} \\ \frac{1}{\sqrt{2}} & 0 & \frac{1}{\sqrt{2}} \end{pmatrix} \begin{pmatrix} 1 \\ 1 \\ 1 \end{pmatrix}$$

This leads to $\sin \alpha_1 \cos \beta_1 = -\frac{\sqrt{2}}{3}$; $\sin \alpha_1 \sin \beta_1 = -\frac{1}{3}$; $\cos \alpha_1 = \frac{\sqrt{2}}{\sqrt{3}}$, and thus to $\alpha_1 = 35^\circ, 3$, $\beta_1 = 215^\circ, 3$.

2.7 Description of an Orientation by Inverse Pole Figures

The reference system of an inverse pole figure is the frame C associated with the crystal and the orientation is defined by the directions of axes connected with the specimen. These axes are usually the axes $\vec{s}_1, \vec{s}_2, \vec{s}_3$ parallel to RD, TD, ND. In analogy to Eq. (31) where the spherical coordinates α_i, β_i of a unit vector R_i parallel to the crystallographic axis (X_i, Y_i, Z_i) have been considered in the system S, here the spherical coordinates γ_i, δ_i of a unit vector \vec{R}_i parallel to a sample axis \vec{s}_i in the coordinate system C must be introduced

$$\vec{R}_i = \vec{s}_i = \sin \gamma_i \cos \delta_i \vec{c}_1 + \sin \gamma_i \sin \delta_i \vec{c}_2 + \cos \delta_i \vec{c}_3. \quad (34)$$

According to Eq. (4) one obtains by scalar multiplication in succession by $\vec{c}_1, \vec{c}_2, \vec{c}_3$

$$g_{1i} = \sin \gamma_i \cos \delta_i; \quad g_{2i} = \sin \gamma_i \sin \delta_i; \quad g_{3i} = \cos \delta_i. \quad (35)$$

These expressions describe the elements of the orientation matrix g in terms of the positions of ND, TD, RD in the inverse pole figure.

2.8 Relationships Between the Different Types of Orientation Parameters

Since all the above matrix representations of an orientation (Eqs. (13), (19), (23), (29)) are equivalent, it is possible to establish the relationships between the different types of orientation parameters by comparing the different types of matrix elements. The most important ones of the resulting relationships are the following:

$$\text{For } (\varphi_1 \phi \varphi_2) \rightleftharpoons (\vartheta \psi \omega) \quad (36)$$

$$\sin \frac{\omega}{2} \sin \vartheta = \sin \frac{\phi}{2}$$

$$\cos \frac{\omega}{2} = \cos \frac{\phi}{2} \cos \frac{\varphi_1 + \varphi_2}{2}$$

$$\psi = \frac{1}{2} (\varphi_1 - \varphi_2).$$

$$\text{For (HKL) [UVW]} \rightarrow (\varphi_1 \phi \varphi_2) \quad (37)$$

$$\text{tg } \phi \cos \varphi_2 = \frac{K}{L}$$

$$\text{tg } \varphi_2 = \frac{H}{K}$$

$$\cos \phi \text{ tg } \varphi_1 = \frac{LW}{KU - HV}$$

$$\text{For (HKL) [UVW]} \rightarrow (\vartheta \psi \omega) \quad (38)$$

$$\text{tg } \psi = \frac{WM - HN}{KN - HV + KU}$$

$$\cos \omega = \frac{1}{2NM} (UM + LU - HW + LN - NM)$$

$$\cos \vartheta \sin \omega = \frac{1}{2NM} (KW - LV - VM).$$

$$\text{For (HKL) [UVW]} \rightarrow \alpha_i \beta_i \quad (39)$$

$$\cos \alpha_i = \frac{1}{PM} (HX_i + KY_i + LZ_i)$$

$$\sin \alpha_i \cos \beta_i = \frac{1}{PN} (UX_i + VY_i + WZ_i)$$

$$\sin \alpha_i \sin \beta_i = \frac{1}{PMN} [(KW - LV)X_i + (LU - HW)Y_i + (HV - KU)Z_i]$$

$$\text{For } (\varphi_1 \phi \varphi_2) \rightarrow \alpha_i \beta_i \quad (40)$$

$$\cos \alpha_i = \frac{1}{P} (X_i \sin \varphi_2 \sin \phi + Y_i \cos \varphi_2 \sin \phi + Z_i \cos \phi)$$

$$\sin \alpha_i \cos \beta_i = \frac{1}{P} [X_i (\cos \varphi_1 \cos \varphi_2 - \sin \varphi_1 \sin \varphi_2 \cos \phi) - Y_i (\cos \varphi_1 \sin \varphi_2 + \sin \varphi_1 \cos \varphi_2 \cos \phi) + Z_i \sin \varphi_1 \sin \phi]$$

$$\sin \alpha_i \sin \beta_i = \frac{1}{P} [X_i (\sin \varphi_1 \cos \varphi_2 + \cos \varphi_1 \sin \varphi_2 \cos \phi) - Y_i (\sin \varphi_1 \sin \varphi_2 - \cos \varphi_1 \cos \varphi_2 \cos \phi) - Z_i \cos \varphi_1 \sin \phi]$$

$$\text{For } (\psi \theta \phi) \rightleftharpoons (\varphi_1 \phi \varphi_2) \quad (41)$$

$$\varphi_1 = \frac{\pi}{2} - \psi$$

$$\phi = \theta$$

$$\varphi_2 = \frac{\pi}{2} - \phi.$$

3. THE ORIENTATION SPACE

3.1 Examples for Various Types of Orientation Spaces

The three parameters describing an orientation can be used as coordinates of a three dimensional orientation space in which each point represents an orientation. Applying different types of orientation parameters and coordinate systems, the orientation space can be formed in many ways.

In Fig. 6 use is made of the rotational coordinates ϑ , ψ , ω . The direction of a radius vector R characterizes the axis of rotation \vec{v} and its length the angle of rotation ω . If one further defines that radius vectors with opposite direction characterize rotations with opposite sense (e.g. that vectors above the equatorial plane characterize counter-clockwise and those below clockwise rotations), a sphere with a radius $R_0 = \pi$ will contain all possible orientations.

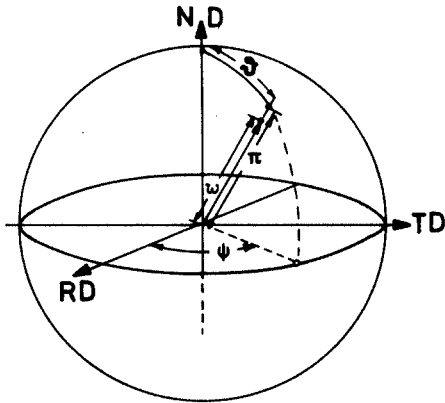


Fig. 6:
Presentation of a spherical orientation space with rotational coordinates \vec{v} , ω .

In Fig. 7 the same parameters ϑ , ψ , ω are applied in another form. The ω -axis (from $-\pi$ to $+\pi$) is chosen as cylinder-axis and the sections $\omega = \text{constant}$ represent the stereographic projection of the axes of rotation \vec{v} . This cylindrical orientation space has proved very useful for describing orientation relationships.

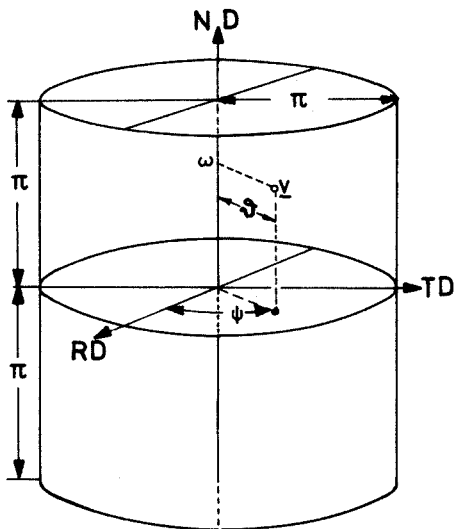


Fig. 7:
Presentation of a cylindrical orientation space with the rotational coordinates \vec{v} , ω .

Most widespread, however, is the use of the orientation space in which the Euler angles φ_1 , ϕ , φ_2 form an Cartesian coordinate system. To present an orientation in this Euler angle space it suffices to consider the range

$$H = \{0 \leq \varphi_1 \leq 2\pi, \quad 0 \leq \phi \leq \pi, \quad 0 \leq \varphi_2 \leq 2\pi\} \quad (42)$$

the so-called asymmetric unit (Fig. 8). This can be recognized in Fig. 5 a where an orientation is characterized by a set of 3 points on the surface of the sphere. By the rotation φ_1 around ND (from 0 to 2π) and by the angle ϕ between ND and [001] (from 0 to π) the position of [001] is determined, whereas φ_2 gives the rotation around [001] (from 0 to 2π).

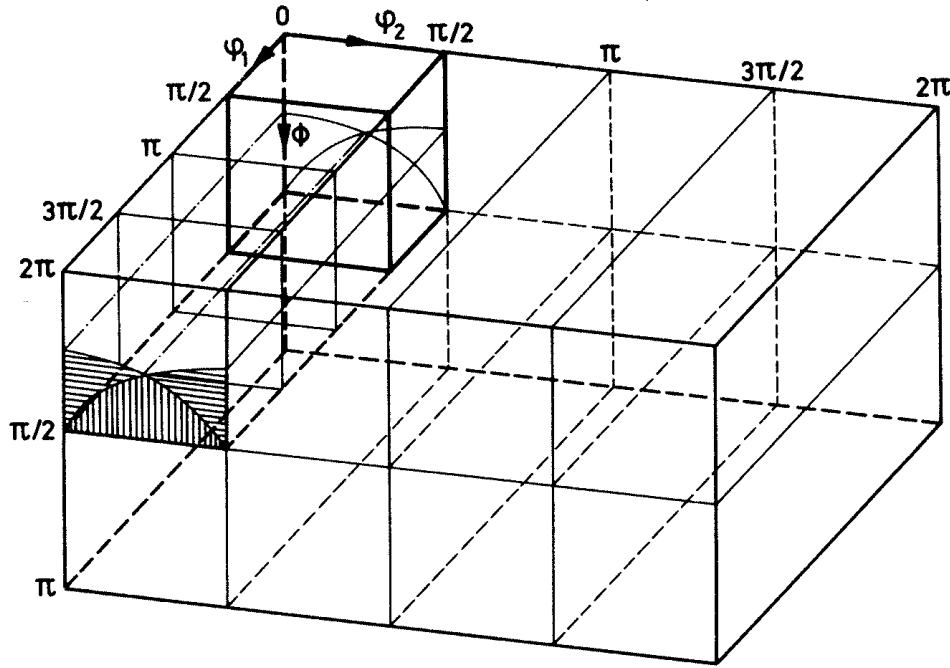


Fig. 8:
Asymmetric unit H of the Euler angle space divided into the subspaces H' and H'' .

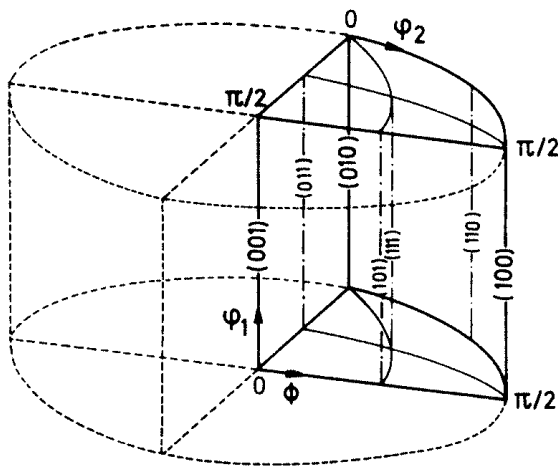


Fig. 9
Presentation of a cylindrical Euler angle space with φ_1 as cylinder axis. The base corresponds to an inverse pole figure.

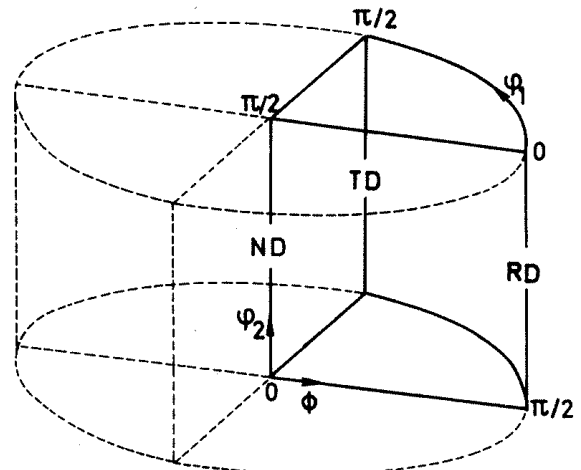


Fig. 10:
Presentation of a cylindrical Euler angle space with φ_2 as cylinder axis. The base corresponds to a pole figure.

Fig. 9 shows a cylindrical type of orientation space based also on the Euler angles φ_1 , ϕ , φ_2 . (For reasons given in Sec. 3.3 only the section $0 \leq \varphi_1, \phi, \varphi_2 \leq \pi/2$ is represented in the figure.) The cylinder axis is put into the direction [001] and the base plane represents a stereographic projection of the ND's thus

corresponding to an inverse pole figure. As follows directly from the definition of the Euler angles, ϕ then gives the pole distance and φ_2 the azimuth of the ND, whereas φ_1 , the rotation around ND, is plotted parallel to the axis. It is often convenient to use this type of Euler angle space together with pole figure considerations. It is possible, of course, to exchange the coordinates φ_1 and φ_2 (Fig. 10). Then an Euler angle space is obtained which is fixed to the sample coordinate system and corresponds to the usual pole figure.

3.2 Symmetrically Equivalent Orientations

If the crystal lattice and/or the specimen (i.e. the pole figure) contain symmetries, orientations which would be different without these symmetries will become symmetrically equivalent. In the case of cubic crystal symmetry, the symmetrically equivalent orientations are found by interchanging the six (equivalent) half axes of the cube. A given half axis can assume six different positions and, for each of these positions by rotation around this half axis, a second half axes four different positions. Under the supposition that only right hand coordinate systems are considered, also the other half axes are determined when these two are fixed so that $6 \cdot 4 = 24$ symmetrically equivalent orientations are obtained (If additionally also left hand systems would be taken into account, altogether 48 possibilities would arise).

In the case of a rolled polycrystalline sheet, the sample axes ND, TD and RD can be interchanged according to the (orthorhombic) symmetry of rolling. E.g. + RD and - RD and, for each of these two positions, also + ND and - ND can be interchanged. Since, considering again only right hand systems, the two TD-half axes are then fixed so that here 4 symmetrically equivalent orientations are obtained. This shows up also the symmetry of the 4 quadrants of the pole figure. Hence, for a rolled sheet of a cubic material, all together $24 \cdot 4 = 96$ orientations are symmetrically equivalent.

These relationships shall now be looked at somewhat closer. Beside the unity element, the elements of point symmetry for crystal and specimen are given by rotation axes and by an inversion. In the following the symbols E and I shall denote the unity and inversion element, L_α^i an i-fold rotation axis parallel to the direction α and T_α a translation in direction of α . The here considered crystal symmetry given by the $G_c = m3m$ group of the cubic system has the symmetry elements I, L_{001}^4 , L_{100}^2 , L_{111}^3 *. For a sample symmetry given by the $G_s = mmm$ group of the orthorhombic system, one has as symmetry elements the axes L_{ND}^2 , L_{RD}^2 and again the inversion I.

The orientations g^c symmetrically equivalent to an orientation g are determined by the relation

$$g^c = g_c \cdot g \cdot g_s \quad (43)$$

where g_c and g_s are the elements of the point symmetry groups G_c and G_s of the crystal and sample. Since the application of an inversion element does not generate symmetrically equivalent orientations (it only converts a left-hand coordinate system into a right-hand one) and since the groups G_c and G_s both contain an inversion I, one can disregard the inversions for our reasoning. It follows from Eq. (43):

$$g^c = I \cdot g \cdot I = g \cdot I \cdot I = g \cdot E = g \quad (44)$$

i.e. the groups G_c and G_s can be thought to be replaced by subgroups G'_c and G'_s not containing I. Thus the here considered group mmm can be replaced by 222 and m3m by 432. The generating elements of the group 432 are the rotation axes L_{001}^4 and L_{111}^3 . Their combination leads to all the 24 symmetry elements ** listed in Table 3.2.

* The L_{100}^2 element is not necessary for the formation of the m3m group, but its consideration is convenient in the deliberations. The three-fold axis can be replaced by another four-fold axis according to $L_{111}^3 = L_{100}^4 \cdot L_{001}^4$. The product of a two-fold axis and the inversion gives a mirror plane $P = IL^2$. From this it follows also that two two-fold axes result in two mirror planes: $L_z^2 \cdot L_x^2 = P_z \cdot P_x$.

** This remark see on page 16.

Table 3.2: The 24 possible symmetry elements of the group 432. Column 1 contains the here applied symbols for the symmetries and column 2 the corresponding matrix representation. Column 3 contains the positions for the orthogonal coordinate axes x , y , z after the symmetry operation has been carried out.

1	2	3
1 E	$\begin{pmatrix} 1 & 0 & 0 \\ 0 & 1 & 0 \\ 0 & 0 & 1 \end{pmatrix}$	$x \ y \ z$
2 L_{010}^2	$\begin{pmatrix} -1 & 0 & 0 \\ 0 & 1 & 0 \\ 0 & 0 & -1 \end{pmatrix}$	$\bar{x} \ y \ \bar{z}$
3 L_{001}^2	$\begin{pmatrix} -1 & 0 & 0 \\ 0 & -1 & 0 \\ 0 & 0 & 1 \end{pmatrix}$	$\bar{x} \ \bar{y} \ z$
4 L_{100}^2	$\begin{pmatrix} 1 & 0 & 0 \\ 0 & -1 & 0 \\ 0 & 0 & -1 \end{pmatrix}$	$x \ \bar{y} \ \bar{z}$
5 L_{111}^3	$\begin{pmatrix} 0 & 1 & 0 \\ 0 & 0 & 1 \\ 1 & 0 & 0 \end{pmatrix}$	$y \ z \ x$
6 $L_{1\bar{1}\bar{1}}^3$	$\begin{pmatrix} 0 & -1 & 0 \\ 0 & 0 & 1 \\ -1 & 0 & 0 \end{pmatrix}$	$\bar{y} \ z \ \bar{x}$
7 $L_{1\bar{1}1}^3$	$\begin{pmatrix} 0 & -1 & 0 \\ 0 & 0 & -1 \\ 1 & 0 & 0 \end{pmatrix}$	$\bar{y} \ \bar{z} \ x$
8 $L_{11\bar{1}}^3$	$\begin{pmatrix} 0 & 1 & 0 \\ 0 & 0 & -1 \\ -1 & 0 & 0 \end{pmatrix}$	$y \ \bar{z} \ \bar{x}$
9 $L_{1\bar{1}\bar{1}}^3$	$\begin{pmatrix} 0 & 0 & 1 \\ 1 & 0 & 0 \\ 0 & 1 & 0 \end{pmatrix}$	$z \ x \ y$
10 $L_{11\bar{1}}^3$	$\begin{pmatrix} 0 & 0 & -1 \\ 1 & 0 & 0 \\ 0 & -1 & 0 \end{pmatrix}$	$\bar{z} \ x \ \bar{y}$
11 L_{111}^3	$\begin{pmatrix} 0 & 0 & -1 \\ -1 & 0 & 0 \\ 0 & 1 & 0 \end{pmatrix}$	$\bar{z} \ \bar{x} \ y$
12 $L_{1\bar{1}1}^3$	$\begin{pmatrix} 0 & 0 & 1 \\ -1 & 0 & 0 \\ 0 & -1 & 0 \end{pmatrix}$	$z \ \bar{x} \ \bar{y}$

1	2	3
13 $L_{10\bar{1}}^2$	$\begin{pmatrix} 0 & 0 & -1 \\ 0 & -1 & 0 \\ -1 & 0 & 0 \end{pmatrix}$	$\bar{z} \ \bar{y} \ \bar{x}$
14 L_{101}^2	$\begin{pmatrix} 0 & 0 & 1 \\ 0 & -1 & 0 \\ 1 & 0 & 0 \end{pmatrix}$	$z \ \bar{y} \ x$
15 L_{010}^4	$\begin{pmatrix} 0 & 0 & 1 \\ 0 & 1 & 0 \\ -1 & 0 & 0 \end{pmatrix}$	$z \ y \ \bar{x}$
16 L_{010}^4	$\begin{pmatrix} 0 & 0 & -1 \\ 0 & 1 & 0 \\ 1 & 0 & 0 \end{pmatrix}$	$\bar{z} \ y \ x$
17 $L_{01\bar{1}}^2$	$\begin{pmatrix} -1 & 0 & 0 \\ 0 & 0 & -1 \\ 0 & -1 & 0 \end{pmatrix}$	$\bar{x} \ \bar{z} \ \bar{y}$
18 L_{100}^4	$\begin{pmatrix} 1 & 0 & 0 \\ 0 & 0 & -1 \\ 0 & 1 & 0 \end{pmatrix}$	$x \ \bar{z} \ y$
19 L_{100}^4	$\begin{pmatrix} 1 & 0 & 0 \\ 0 & 0 & 1 \\ 0 & -1 & 0 \end{pmatrix}$	$x \ z \ \bar{y}$
20 L_{011}^2	$\begin{pmatrix} -1 & 0 & 0 \\ 0 & 0 & 1 \\ 0 & 1 & 0 \end{pmatrix}$	$\bar{x} \ z \ y$
21 L_{110}^2	$\begin{pmatrix} 0 & -1 & 0 \\ -1 & 0 & 1 \\ 0 & 0 & -1 \end{pmatrix}$	$\bar{y} \ \bar{x} \ \bar{z}$
22 L_{001}^4	$\begin{pmatrix} 0 & 1 & 0 \\ -1 & 0 & 0 \\ 0 & 0 & 1 \end{pmatrix}$	$y \ \bar{x} \ z$
23 L_{110}^2	$\begin{pmatrix} 0 & 1 & 0 \\ 1 & 0 & 0 \\ 0 & 0 & -1 \end{pmatrix}$	$y \ x \ \bar{z}$
24 $L_{00\bar{1}}^4$	$\begin{pmatrix} 0 & -1 & 0 \\ 1 & 0 & 0 \\ 0 & 0 & 1 \end{pmatrix}$	$\bar{y} \ x \ z$

Table 3.2: The 24 possible symmetry elements of the group 432. Column 1 contains the here applied symbols for the symmetries and column 2 the corresponding matrix representation. Column 3 contains the positions for the orthogonal coordinate axes x, y, z after the symmetry operation has been carried out.

1	2	3
1 E	$\begin{pmatrix} 1 & 0 & 0 \\ 0 & 1 & 0 \\ 0 & 0 & 1 \end{pmatrix}$	$x \ y \ z$
2 L_{010}^2	$\begin{pmatrix} -1 & 0 & 0 \\ 0 & 1 & 0 \\ 0 & 0 & -1 \end{pmatrix}$	$\bar{x} \ y \ \bar{z}$
3 L_{001}^2	$\begin{pmatrix} -1 & 0 & 0 \\ 0 & -1 & 0 \\ 0 & 0 & 1 \end{pmatrix}$	$\bar{x} \ \bar{y} \ z$
4 L_{100}^2	$\begin{pmatrix} 1 & 0 & 0 \\ 0 & -1 & 0 \\ 0 & 0 & -1 \end{pmatrix}$	$x \ \bar{y} \ \bar{z}$
5 L_{111}^3	$\begin{pmatrix} 0 & 1 & 0 \\ 0 & 0 & 1 \\ 1 & 0 & 0 \end{pmatrix}$	$y \ z \ x$
6 $L_{1\bar{1}\bar{1}}^3$	$\begin{pmatrix} 0 & -1 & 0 \\ 0 & 0 & 1 \\ -1 & 0 & 0 \end{pmatrix}$	$\bar{y} \ z \ \bar{x}$
7 $L_{1\bar{1}1}^3$	$\begin{pmatrix} 0 & -1 & 0 \\ 0 & 0 & -1 \\ 1 & 0 & 0 \end{pmatrix}$	$\bar{y} \ \bar{z} \ x$
8 $L_{11\bar{1}}^3$	$\begin{pmatrix} 0 & 1 & 0 \\ 0 & 0 & -1 \\ -1 & 0 & 0 \end{pmatrix}$	$y \ \bar{z} \ \bar{x}$
9 $L_{1\bar{1}\bar{1}}^3$	$\begin{pmatrix} 0 & 0 & 1 \\ 1 & 0 & 0 \\ 0 & 1 & 0 \end{pmatrix}$	$z \ x \ y$
10 $L_{11\bar{1}}^3$	$\begin{pmatrix} 0 & 0 & -1 \\ 1 & 0 & 0 \\ 0 & -1 & 0 \end{pmatrix}$	$\bar{z} \ x \ \bar{y}$
11 L_{111}^3	$\begin{pmatrix} 0 & 0 & -1 \\ -1 & 0 & 0 \\ 0 & 1 & 0 \end{pmatrix}$	$\bar{z} \ \bar{x} \ y$
12 $L_{1\bar{1}1}^3$	$\begin{pmatrix} 0 & 0 & 1 \\ -1 & 0 & 0 \\ 0 & -1 & 0 \end{pmatrix}$	$z \ \bar{x} \ \bar{y}$

1	2	3
13 $L_{10\bar{1}}^2$	$\begin{pmatrix} 0 & 0 & -1 \\ 0 & -1 & 0 \\ -1 & 0 & 0 \end{pmatrix}$	$\bar{z} \ \bar{y} \ \bar{x}$
14 L_{101}^2	$\begin{pmatrix} 0 & 0 & 1 \\ 0 & -1 & 0 \\ 1 & 0 & 0 \end{pmatrix}$	$z \ \bar{y} \ x$
15 L_{010}^4	$\begin{pmatrix} 0 & 0 & 1 \\ 0 & 1 & 0 \\ -1 & 0 & 0 \end{pmatrix}$	$z \ y \ \bar{x}$
16 L_{010}^4	$\begin{pmatrix} 0 & 0 & -1 \\ 0 & 1 & 0 \\ 1 & 0 & 0 \end{pmatrix}$	$\bar{z} \ y \ x$
17 $L_{01\bar{1}}^2$	$\begin{pmatrix} -1 & 0 & 0 \\ 0 & 0 & -1 \\ 0 & -1 & 0 \end{pmatrix}$	$\bar{x} \ \bar{z} \ \bar{y}$
18 L_{100}^4	$\begin{pmatrix} 1 & 0 & 0 \\ 0 & 0 & -1 \\ 0 & 1 & 0 \end{pmatrix}$	$x \ \bar{z} \ y$
19 L_{100}^4	$\begin{pmatrix} 1 & 0 & 0 \\ 0 & 0 & 1 \\ 0 & -1 & 0 \end{pmatrix}$	$x \ z \ \bar{y}$
20 L_{011}^2	$\begin{pmatrix} -1 & 0 & 0 \\ 0 & 0 & 1 \\ 0 & 1 & 0 \end{pmatrix}$	$\bar{x} \ z \ y$
21 L_{110}^2	$\begin{pmatrix} 0 & -1 & 0 \\ -1 & 0 & 1 \\ 0 & 0 & -1 \end{pmatrix}$	$\bar{y} \ \bar{x} \ \bar{z}$
22 L_{001}^4	$\begin{pmatrix} 0 & 1 & 0 \\ -1 & 0 & 0 \\ 0 & 0 & 1 \end{pmatrix}$	$y \ \bar{x} \ z$
23 L_{110}^2	$\begin{pmatrix} 0 & 1 & 0 \\ 1 & 0 & 0 \\ 0 & 0 & -1 \end{pmatrix}$	$y \ x \ \bar{z}$
24 $L_{00\bar{1}}^4$	$\begin{pmatrix} 0 & -1 & 0 \\ 1 & 0 & 0 \\ 0 & 0 & 1 \end{pmatrix}$	$\bar{y} \ x \ z$

$$[L_c^i L_s^j] = \begin{pmatrix} \Delta\varphi_1 \\ \Delta\phi \\ \Delta\varphi_2 \end{pmatrix} + \begin{pmatrix} \pm 1 & 0 & 0 \\ 0 & \pm 1 & 0 \\ 0 & 0 & \pm 1 \end{pmatrix}. \quad (51)$$

Before considering the effect of the different symmetry elements of crystal and sample in detail (Sec. 3.4 to 3.6), the symmetries of the Euler angle space induced by identical equivalencies will be briefly discussed.

3.3 Symmetries of the Euler Angle Space due to Identical Equivalencies

As shown in Sec. 2.3 the matrix elements g_{ik} may assume the same values for different sets of Euler angles $\varphi_1 \phi \varphi_2$. Since the rotation between the two frames C and S is completely defined by the matrix g , different sets of Euler angles leading to the same matrix are called identically equivalent orientations.

Such identically equivalent orientations are defined by the equation

$$g(\varphi_1^e \phi^e \varphi_2^e) = g(\varphi_1 \phi \varphi_2). \quad (52)$$

It is easy to recognize that the solution of this equation which is given by Eq. (20) can be expressed as a linear transformation of the form of Eq. (46)

$$\epsilon^e = \begin{pmatrix} \varphi_1^e \\ \phi^e \\ \varphi_2^e \end{pmatrix} = \begin{pmatrix} \pi \\ 0 \\ \pi \end{pmatrix} + \begin{pmatrix} 1 & 0 & 0 \\ 0 & -1 & 0 \\ 0 & 0 & 1 \end{pmatrix} \begin{pmatrix} \varphi_1 \\ \phi \\ \varphi_2 \end{pmatrix} = \begin{pmatrix} \pi \\ 0 \\ \pi \end{pmatrix} + P_\phi \cdot \epsilon. \quad (53)$$

This means one has in the Euler angle space a mirror plane P_ϕ perpendicular to the axis ϕ in $\phi = 0$ superimposed by a translation $\Delta\varphi_1 = \pi$, $\Delta\phi = 0$ and $\Delta\varphi_2 = \pi$, i.e. one has a glide-mirror plane. Since Eq. (52) can be derived from Eq. (45) by setting $g_c = g_s = E$, Eq. (53) can also be written in an operator notation of Eq. (48) as

$$[E, E] = \begin{pmatrix} \pi \\ 0 \\ \pi \end{pmatrix} + P_\phi. \quad (54)$$

As also pointed out in Sec. 2.3, further solutions of Eq. (52), i.e. further identical equivalencies, are obtained by translations by multiples of 2π parallel to each of the axes $\varphi_1, \phi, \varphi_2$. As can easily be recognized and is indicated in Fig. 11, this leads to a family of glide-mirror planes perpendicular to the ϕ -axis in $\phi = k\pi$ with translation components $(2k_1 + 1)\pi$ and $(2k_2 + 1)\pi$ parallel to the axes φ_1 and φ_2 with k, k_1, k_2 being integers. Thus the symmetries induced by the identical equivalencies imply a division of the Euler angle space into equivalent regions. These can be chosen in different ways. Here the range

$$H = \{ 0 \leq \varphi_1 \leq 2\pi, \quad 0 \leq \phi \leq \pi, \quad 0 \leq \varphi_2 \leq 2\pi \}. \quad (55)$$

(Eq. (42) and Fig. 11) is chosen as the basic range and will be referred to as asymmetric unit (c.f. /7/).

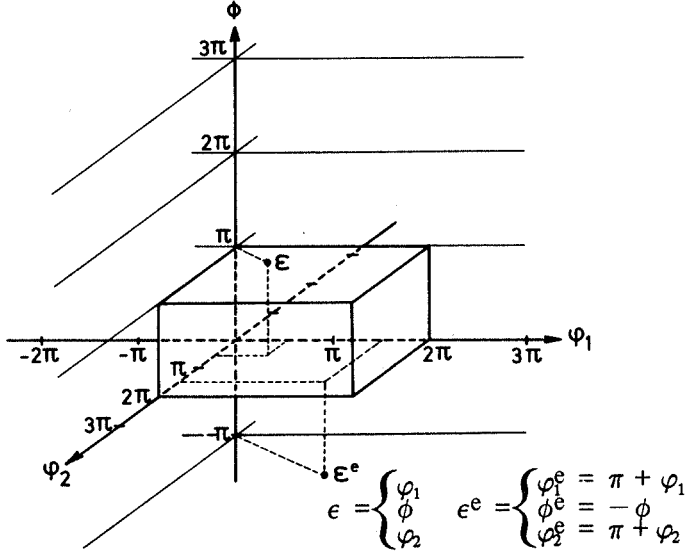


Fig. 11:
Glide mirror planes in the infinite Euler angle space induced by identical equivalences. They divide the space into identically equivalent subspaces, one of them being the asymmetric unit H.

3.4 Symmetries of the Euler Angle Space Induced by the Cubic Crystal Symmetry

Now let us consider the effect of the cubic crystal symmetry. Using the form of writing given by Eq. (51) the elements L_{100}^2 and L_{001}^4 give /7/,

$$(I) \quad [L_{100}^2, E] = \begin{pmatrix} \pi \\ \pi \\ \pi \end{pmatrix} + \begin{pmatrix} 1 & 0 & 0 \\ 0 & -1 & 0 \\ 0 & 0 & -1 \end{pmatrix} = \begin{pmatrix} \pi \\ \pi \\ \pi \end{pmatrix} + L_{\varphi_1}^2 \quad (56)$$

$$(II) \quad [L_{001}^4, E] = \begin{pmatrix} \pi/2 \\ \pi/2 \\ \pi/2 \end{pmatrix} + \begin{pmatrix} 1 & 0 & 0 \\ 0 & 1 & 0 \\ 0 & 0 & 1 \end{pmatrix} = \begin{pmatrix} 0 \\ 0 \\ \pi/2 \end{pmatrix} + E$$

Combining I and II on the basis of formulae (49): leads to

$$(III) \quad [L_{100}^2 \cdot L_{001}^4, E] = [L_{100}^2, E] \cdot [L_{001}^4, E] = \begin{pmatrix} \pi \\ \pi \\ \pi/2 \end{pmatrix} + L_{\varphi_1}^2. \quad (57)$$

The resulting symmetry elements for the range H of the Euler angle space are shown in Fig. 12 a–c. One recognizes that L_{100}^2 induces two-fold screw axes $L_{\varphi_1}^2 + (\Delta\varphi_1 = \pi)$ parallel to φ_1 with a translation vector of $\Delta\varphi_1 = \pi$ and the coordinates

$$\phi^0 = \frac{\Delta\phi}{2} = \frac{\pi}{2}; \quad \varphi_2^0 = \frac{\Delta\varphi_2}{2} = \frac{\pi}{2} \quad \text{and} \quad \phi^0 = \frac{\Delta\phi}{2} = \frac{\pi}{2}; \quad \varphi_2^0 = \frac{\Delta\varphi_2 + 2\pi}{2} = \frac{3\pi}{2}.$$

By these axes a point a is brought into the position b (Fig. 12 d).

The L_{001}^4 axis induces a translation vector $\Delta\varphi_2 = \pi/2$, that is, a periodicity of $\pi/2$ for the angle φ_2 (Fig. 12 b). This translation converts a point a into the position a' and b into b'. Combined, the two elements L_{100}^2 and L_{001}^4 introduce a family of two-fold screw axes $L_{\varphi_2}^2 + (\Delta\varphi_1 = \pi)$ having the coordinates $\phi^0 = \pi/2, \varphi_2^0 = 0, \pi/4, 2\pi/4 \dots 8\pi/4$, which transform the point b' back into the original position a. Thus these symmetries $[L_{100}^2, E]$ and $[L_{001}^4, E]$ allow the region H to be divided into $2 \cdot 4 = 8$ symmetrically equivalent subregions. Here mainly the subregion

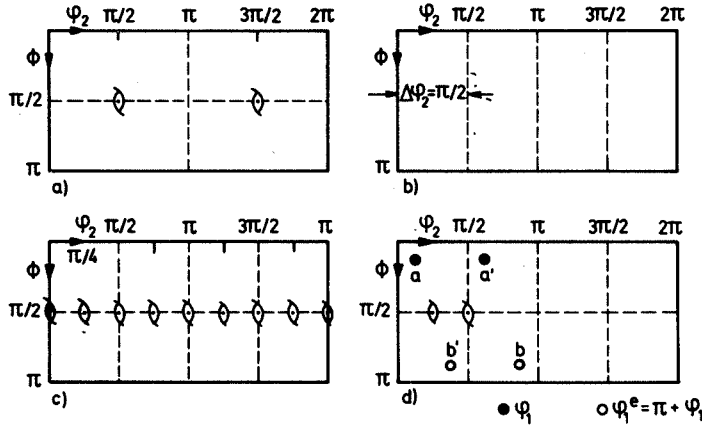


Fig. 12:
Symmetry elements in the Euler angle space induced by the cubic crystal symmetry. Fig. 12 d illustrates the transformation effected by these elements.

$$H' = \{ 0 \leq \varphi_1 \leq 2\pi, \quad 0 \leq \phi \leq \pi/2, \quad 0 \leq \varphi_2 \leq \pi/2 \} \quad (58)$$

(Fig. 8) will be considered.

The remaining three-fold axis L_{111}^3 causes a non-linear transformation which cannot be expressed by elements of space symmetry in the Euler angle space. It causes a quasi three-fold screw axis parallel to φ_1 having the coordinates $\phi^0 = \arccos(1/\sqrt{3})$, $\varphi_2^0 = \pi/4$ (Q^3 in Fig. 13).

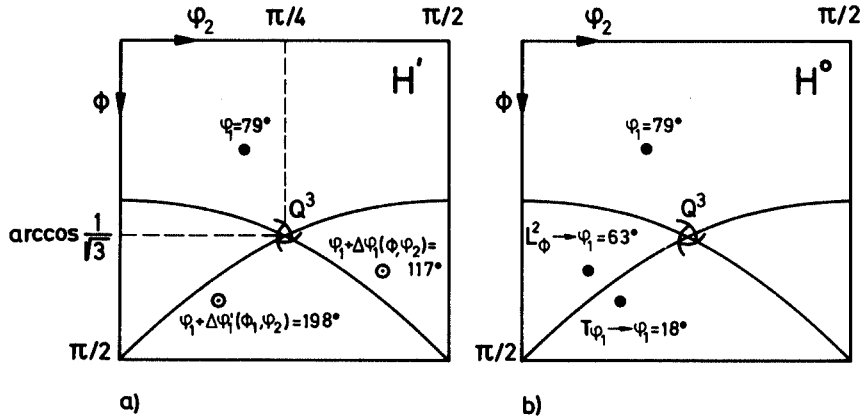


Fig. 13:
Position and effect of the quasi-screw axis Q^3 induced by the three-fold crystal axis: a) in the subspace H' ; b) in the subspace H^0 .

It effects that a point lying on this axis is shifted along this axis by $\Delta\varphi_1' = 120^\circ$ or $\Delta\varphi_1'' = 240^\circ$ and that a point lying beside it (i.e. having the coordinates $\phi, \varphi_2 \neq \phi^0, \varphi_2^0$) is displaced screw-wise into two other positions ϕ_1', ϕ_2' and ϕ_1'', ϕ_2'' . The new coordinates $\phi_1', \phi_2', \phi_1'', \phi_2''$ as well as the shifts $\Delta\varphi_1 = \varphi_1' - \varphi_1$ and $\Delta\varphi_1' = \varphi_1'' - \varphi_1$ depend only on the coordinates ϕ, φ_2 , but not on φ_1 . Thus a segment parallel to φ_1 remains parallel to φ_1 and conserves its length at this transformation (Fig. 13).

This transformation described by the quasi-three-fold axis divides the range H' into three symmetrically equivalent parts. It thus follows that the cubic crystal symmetry induce into the orientation space H $2 \cdot 4 \cdot 3 = 24$ symmetrical equivalences for orientations, thereby dividing the range H into 24 basic ranges.

There are many possible choices of surface limiting the basic regions which all are plane except those which follow from the three-fold axis. A simple possibility is to divide the range H' into three right prisms of height $\varphi_1 = 2\pi$. Their cross section in the plane perpendicular to the φ_1 axis is shown in Fig. 14, where

the three basic areas are indicated by different types of hatching. Thus for cubic single crystals one of the 3 prismatic regions would be needed for representing every possible orientation once and only once.

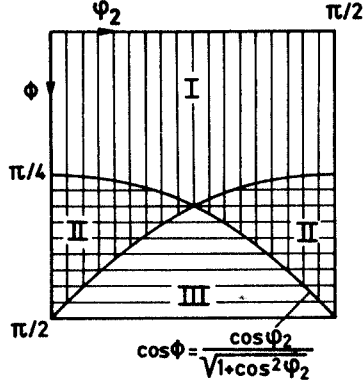


Fig. 14:
Division of the subspaces H' and H° into three symmetrically equivalent subspaces by the three-fold crystal symmetry.

3.5 Symmetries of the Euler Angle Space in the Case of Orthorhombic Sample Symmetry

Now let us consider orthorhombic symmetry for the sample and thus the effect of the elements L_{ND}^2 and L_{RD}^2 . They induce symmetries into the Euler angle space which are indicated in Fig. 15 for the range H [7]:

$$(IV) [E, L_{ND}^2] = \begin{pmatrix} \pi \\ 0 \\ 0 \end{pmatrix} + \begin{pmatrix} 1 & 0 & 0 \\ 0 & 1 & 0 \\ 0 & 0 & 1 \end{pmatrix} = \begin{pmatrix} \pi \\ 0 \\ 0 \end{pmatrix} + E \quad (59)$$

$$(V) [E, L_{RD}^2] = \begin{pmatrix} \pi \\ \pi \\ \pi \end{pmatrix} + \begin{pmatrix} -1 & 0 & 0 \\ 0 & -1 & 0 \\ 0 & 0 & 1 \end{pmatrix} = \begin{pmatrix} \pi \\ \pi \\ \pi \end{pmatrix} + L_{\varphi_2}^2 \quad (60)$$

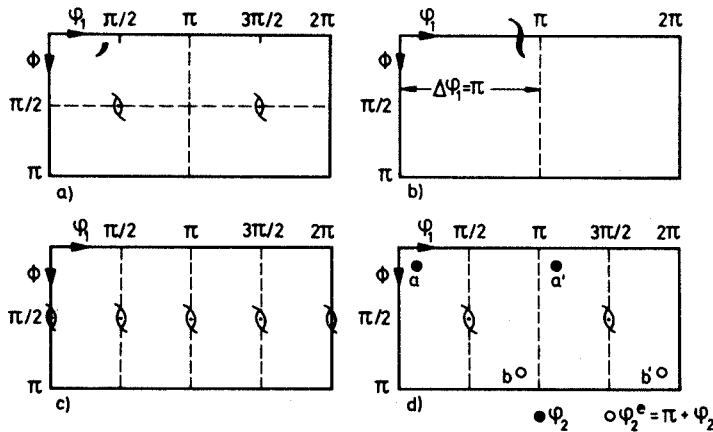


Fig. 15:
Symmetry elements in the Euler angle space induced by the orthorhombic sample symmetry. Fig. 15 d illustrates the transformation effected by these elements.

One recognizes that the axis L_{ND}^2 induces into the orientation space the translation $\Delta\varphi_1 = \pi$, i.e. the periodicity π for φ_1 which transforms a point a into the position a' . The element L_{RD}^2 induces a two-fold screw axis $L_{\varphi_2}^2 + (\Delta\varphi_2 = \pi)$ having the coordinates $\varphi^\circ = \pi/2$, $\varphi_1 = \pi/2, 3\pi/2$. It transforms a into the position b and a' into b' . It can easily be seen that the elements L_{ND}^2 and L_{RD}^2 introduce a division of the range H' into yet another $2 \cdot 2 = 4$ symmetrically equivalent subregions with intersection planes perpendicular to φ_1 at the points $\varphi_1 = \pi/2, \pi, 3\pi/2$.

Interesting is the combination with the crystal symmetry elements. The translation $\Delta\varphi_1 = \pi$ generated by the axis L_{ND}^2 transforms the two-fold screw axis $L_{\varphi_1}^2 + (\Delta\varphi_1 = \pi)$ introduced by the element L_{100}^2 into an ordinary two-fold axis $L_{\varphi_1}^2$. This also follows from Eqs. (49) and (57):

$$(VI) [L_{100}^2 \cdot L_{001}^4, L_{ND}^2] = [L_{100}^2 \cdot L_{001}^4, E] \cdot [E, L_{ND}^2] = \begin{pmatrix} 0 \\ \pi \\ \pi/2 \end{pmatrix} + L_{\varphi_1}^2. \quad (61)$$

Similarly, with Eqs. (57) and (60), L_{RD}^2 leads to a translation in the φ_2 -direction and a two-fold axis parallel ϕ :

$$(VII) [L_{100}^2 \cdot L_{001}^4, L_{RD}^2] = [L_{100}^2 \cdot L_{001}^4, E] \cdot [E, L_{RD}^2] = \begin{pmatrix} 0 \\ 0 \\ \pi/2 \end{pmatrix} + L_{\phi}^2. \quad (62)$$

Finally, the combination of L_{ND}^2 and L_{RD}^2 results in

$$(VIII) [L_{100}^2 \cdot L_{001}^4, L_{ND}^2 \cdot L_{RD}^2] = [L_{100}^2 \cdot L_{001}^4, L_{ND}^2] \cdot [E, L_{RD}^2] = \begin{pmatrix} \pi \\ 0 \\ \pi/2 \end{pmatrix} + L_{\phi}^2. \quad (63)$$

This gives a family of two-fold axes parallel to ϕ having the coordinates $\varphi_1^0 = 0, \pi/2, 2\pi/2 \dots$; $\varphi_2^0 = 0, \pi/4, 2\pi/4 \dots$

As already pointed out, the transformation introduced by the three-fold axis L_{111}^3 of the crystal symmetry cannot be described by space symmetry elements in the Euler angle space. It introduces, however, some two- and one-dimensional symmetries within special planes and along special lines. One finds in the planes $\varphi_2 = n\pi/2$ ($n = 0, \pm 1, \pm 2 \dots$)

$$[L_{001}^4 \cdot L_{111}^3, L_{ND}^2]_{\varphi_2 = n\pi/2} = \begin{cases} \varphi_1^e = \varphi_1 \\ \phi^e = \pi/2 - \phi \end{cases} = \begin{pmatrix} 0 \\ 0 \\ \pi/2 \end{pmatrix} + L^M. \quad (64)$$

i.e. in these planes there is a line parallel to φ_1 at $\phi = \pi/4$, which can be called a mirror line L^M . Furthermore, along the lines (called l) parallel to φ_1 at $\phi = 0, \varphi_2 = 0, \pi/2$ and $\phi = \pi/2, \varphi_2 = 0, \pi/2$ one has

$$[L_{111}^3 \cdot L_{001}^4, L_{ND}^2 \cdot L_{RD}^2]_l = \left\{ \varphi_1^e = \frac{\pi}{2} - \varphi_1 \right\} = \begin{pmatrix} \pi \\ 2 \end{pmatrix} + L^P \quad (65)$$

i.e. along these lines at $\varphi_1 = \pi/2$ points are situated which can be called mirror points L^P . Further mirror points along the axis Q^3 ($\phi = \arccos(1/\sqrt{3})$, $\varphi_2 = \pi/4$) follow from

$$[L_{001}^4 \cdot L_{100}^2 \cdot L_{111}^3, L_{ND}^2 \cdot L_{RD}^2]_{Q^3} = \left\{ \varphi_1^e = k\frac{\pi}{3} - \varphi_1 \right\} = \begin{pmatrix} \pi \\ 3 \end{pmatrix} + L^P \quad (66)$$

and are situated at $\varphi_1 = \frac{1}{2} \gamma \frac{\pi}{3}$ ($\gamma = 0, \pm 1, \pm 2 \dots$) *. In the above, the operators L^M and L^P have the meaning

* The points on Q^3 at $\varphi_1 = \gamma\pi/2$ are situated on two-fold axes and cause the same symmetry operations along the line Q^3 as these axes. Thus, in contrast to the other mirror points along Q^3 , these ones are no true additional symmetry elements.

$$L^M = \begin{pmatrix} 1 & 0 \\ 0 & -1 \end{pmatrix}; \quad L^P = (-1).$$

The description of symmetries in the Euler angle space given in this section is complete within the range H . These symmetries, however, give no possibility of transforming of orientations from the range $0 \leq \phi \leq \pi$ considered here to the neighbouring ranges $-\pi \leq \phi \leq 0$ or $\pi \leq \phi \leq 2\pi$. This possibility is obtained only by combining the symmetries induced by the rotation axes with those induced by the glide-mirror plane and given by Eq. (54). Using Eq. (54) and /7/ it can be shown that in the present case the translation $\Delta\varphi_1 = \pi$ and $\Delta\varphi_2 = \pi$ introduced by the axis L_{ND}^2 or L_{001}^4 , respectively, reduce the glide-mirror plane into a simple mirror plane:

$$\begin{pmatrix} \pi \\ 0 \\ \pi \end{pmatrix} + P_\phi \Rightarrow \begin{pmatrix} 0 \\ 0 \\ 0 \end{pmatrix} + P_\phi.$$

This mirror plane is perpendicular to the axis ϕ in $\phi = 0$. Considering also the translations 2π parallel to the axis ϕ leads to a family of mirror planes perpendicular to the axis ϕ in $\phi = k\pi$ ($k = 0, \pm 1, \pm 2 \dots$).

Recapitulating, we find that the symmetries of the cubic system of the crystal and the orthorhombic system of the sample induces into Euler angle space symmetries corresponding to linear transformations which are listed in Table 3.5. The symmetries 1 to 4 divide the H region into $2 \cdot 4 \cdot 2 \cdot 2 = 32$ symmetrically equivalent subregions. One of them,

$$H^\circ = \{ 0 \leq \varphi_1 \leq \pi/2, 0 \leq \phi \leq \pi/2, 0 \leq \varphi_2 \leq \pi/2 \} \quad (67)$$

having the form of a cube with edge length 90° is depicted in Fig. 16 with the outlined symmetry elements. Due to the three-fold axis L_{111}^3 in the crystal's symmetry, the subregion H° becomes divided further into three symmetrically equivalent parts denoted in Figs. 14 by the numerals I, II, III.

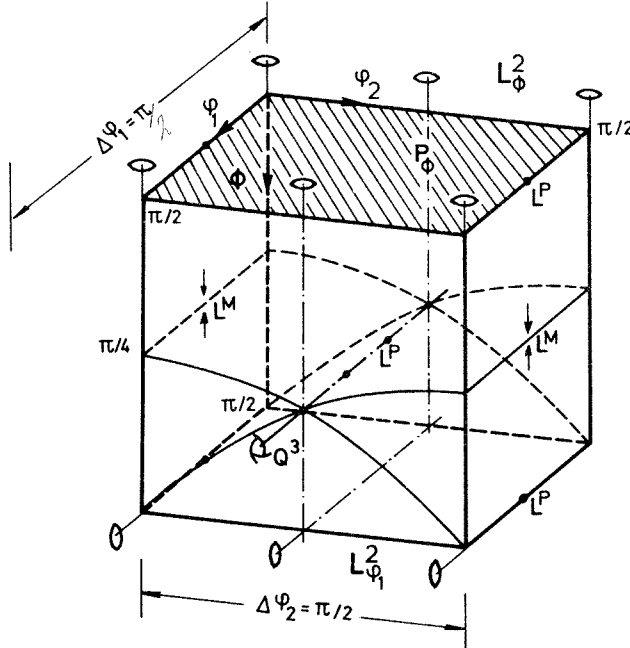


Fig. 16:
Presentation of the symmetry elements in the subspace H° of the Euler angle space.

Table 3.5: Symmetry elements in the Eulers angle space for different sample symmetries (in the triclinic and monoclinic case only the true space symmetries are listed, i.e. Mirror lines and mirror points are omitted).

Triclinic	Orthorhombic
<p>1. translation $\Delta\varphi_2 = \pi/2$</p> $\begin{pmatrix} 0 \\ 0 \\ \pi/2 \end{pmatrix} + E \quad \begin{aligned} \varphi_1^e &= \varphi_1 \\ \phi^e &= \phi \\ \varphi_2^e &= \varphi_2 + \pi/2 \end{aligned}$ <p>2. two-fold screw axis</p> $\begin{pmatrix} \pi \\ \pi \\ \pi/2 \end{pmatrix} + L_{\varphi_1}^2 \quad \begin{aligned} \varphi_1^e &= \pi + \varphi_1 \\ \phi^e &= \pi - \phi \\ \varphi_2^e &= \pi/2 - \varphi_2 \end{aligned}$ <p>3. glide-mirror plane</p> $\begin{pmatrix} \pi \\ 0 \\ 0 \end{pmatrix} + P_\phi \quad \begin{aligned} \varphi_1^e &= \pi + \varphi_1 \\ \phi^e &= -\phi \\ \varphi_2^e &= \varphi_2 \end{aligned}$	<p>1. translation $\Delta\varphi_1 = \pi$</p> $\begin{pmatrix} \pi \\ 0 \\ 0 \end{pmatrix} + E \quad \begin{aligned} \varphi_1^e &= \varphi_1 + \pi \\ \phi^e &= \phi \\ \varphi_2^e &= \varphi_2 \end{aligned}$ <p>2. translation $\Delta\varphi_2 = \pi/2$</p> $\begin{pmatrix} 0 \\ 0 \\ \pi/2 \end{pmatrix} + E \quad \begin{aligned} \varphi_1^e &= \varphi_1 \\ \phi^e &= \phi \\ \varphi_2^e &= \varphi_2 + \pi/2 \end{aligned}$ <p>3. two-fold axis</p> $\begin{pmatrix} 0 \\ \pi \\ \pi/2 \end{pmatrix} + L_{\varphi_1}^2 \quad \begin{aligned} \varphi_1^e &= \varphi_1 \\ \phi^e &= \pi - \phi \\ \varphi_2^e &= \pi/2 - \varphi_2 \end{aligned}$ <p>4. two-fold axis</p> $\begin{pmatrix} \pi \\ 0 \\ \pi/2 \end{pmatrix} + L_\phi^2 \quad \begin{aligned} \varphi_1^e &= \pi - \varphi_1 \\ \phi^e &= \phi \\ \varphi_2^e &= \pi/2 - \varphi_2 \end{aligned}$ <p>5. mirror plane</p> $\begin{pmatrix} 0 \\ 0 \\ 0 \end{pmatrix} + P_\phi \quad \begin{aligned} \varphi_1^e &= \varphi_1 \\ \phi^e &= -\phi \\ \varphi_2^e &= \varphi_2 \end{aligned}$ <p>6. mirror line</p> $\begin{pmatrix} 0 \\ \pi/2 \end{pmatrix} + L^M \quad \begin{aligned} \varphi_1^e &= \varphi_1 \\ \phi^e &= \pi/2 - \phi \\ \varphi_2^e &= 0 \end{aligned}$ <p>7. mirror point</p> $(\pi/2) + L^P \quad \begin{aligned} \varphi_1^e &= \pi/2 - \varphi_1 \\ \phi^e &= 0, \pi/2 \\ \varphi_2^e &= 0, \pi/2 \end{aligned}$ <p>8. mirror point</p> $(\pi/3) + L^P \quad \begin{aligned} \varphi_1^e &= k\pi/3 - \varphi_1 \\ \phi^e &= \arccos 1/\sqrt{3} \\ \varphi_2^e &= \pi/4 \\ (k &= 0, 1, 2 \dots) \end{aligned}$
Monoclinic	
<p>1. translation $\Delta\varphi_2 = \pi/2$</p> $\begin{pmatrix} 0 \\ 0 \\ \pi/2 \end{pmatrix} + E \quad \begin{aligned} \varphi_1^e &= \varphi_1 \\ \phi^e &= \phi \\ \varphi_2^e &= \varphi_2 + \pi/2 \end{aligned}$ <p>2. two-fold screw axis</p> $\begin{pmatrix} \pi \\ \pi \\ \pi/2 \end{pmatrix} + L_{\varphi_1}^2 \quad \begin{aligned} \varphi_1^e &= \pi + \varphi_1 \\ \phi^e &= \pi - \phi \\ \varphi_2^e &= \pi/2 - \varphi_2 \end{aligned}$ <p>3. two-fold axis</p> $\begin{pmatrix} 0 \\ 0 \\ \pi/2 \end{pmatrix} + L_\phi^2 \quad \begin{aligned} \varphi_1^e &= -\varphi_1 \\ \phi^e &= \phi \\ \varphi_2^e &= \pi/2 - \varphi_2 \end{aligned}$ <p>4. glide-mirror plane</p> $\begin{pmatrix} \pi \\ 0 \\ 0 \end{pmatrix} + P_\phi \quad \begin{aligned} \varphi_1^e &= \pi + \varphi_2 \\ \phi^e &= -\phi \\ \varphi_2^e &= \varphi_2 \end{aligned}$	

3.6 Symmetries of the Euler Angle Space in the Case of Lower Sample Symmetry

In the following some cases shall be briefly discussed for which the cubic crystal symmetry is retained, but the sample symmetry is less than orthorhombic. If, for example, the sample is a single crystal, its symmetry (i.e. also that of the pole figure) is given in general by the triclinic group $\bar{1}$ containing only the inversion I . Only if the crystal is oriented in such a way that symmetry axes of the crystal are parallel to ND, RD oder TD, a higher sample symmetry is obtained. A crystal in cube orientation $\{001\}$ $\langle 100 \rangle$ or Goss orientation $\{011\}$ $\langle 100 \rangle$ possesses the orthorhombic, or a crystal in the brass rolling orientation $\{011\}$ $\langle 211 \rangle$ the monoclinic sample symmetry.

For triclinic sample symmetry it is necessary to use the subregion H' (Eq. (58), Fig. 8) instead of H° . Since for each single crystal orientation H' contains three symmetrically equivalent positions (which have distances $> \pi/2$ in φ_1 [7]) and since H' can be divided into 4 regions of the size H° , only 3 of these 4 regions would contain such a position. This means not all crystal orientations would be contained in the range H° used for polycrystals. If, however, it is allowed to rotate the crystal by 180° around RD, TD or ND, one can always manage to have one position in H° . In these cases one can use H° also for the presentation of single crystal orientations. In other cases, e.g. if the orientation relationship with respect to a second crystal is considered, it might not be allowed to think the first crystal being rotated. Then the larger region H' must be used.

In the case of uni-directional rolling (e.g. of sheets or tubes) monoclinic sample symmetry is obtained. One has here the symmetry group m characterized by the inversion I and the two fold-axis L_{RD} . As shown in Sec. 3.5, this axis causes 2-fold screw axes parallel φ_2 in the Euler angle space situated at $\varphi_1 = \pi/2, 3\pi/2$ and $\phi = \pi/2$ (Eq. (60)). This leads to reduction of the range H' into two parts of which one is given by

$$H'' = \left\{ 0 \leq \varphi_1 \leq \pi, \quad 0 \leq \phi, \quad \varphi_2 \leq \frac{\pi}{2} \right\}. \quad (68)$$

In combination with the elements induced by the cubic crystal symmetry, this axis gives ordinary two-fold axes parallel ϕ situated at $\varphi_1 = 0, 2\pi$ and $\varphi_2 = \pi/4$ (Eq. (62)).

4. REPRESENTATION OF ORIENTATION DISTRIBUTIONS IN THE EULER ANGLE SPACE

4.1 The Orientation Distribution Function (ODF)

For a random orientation distribution the density of orientation points in the (linear) Euler angle space would come out not to be constant but would change proportional to $1/\sin \phi$ [8]. For the purpose of representing orientation distributions, however, a function $f(g)$ must be defined in such a manner that $f(g)dg$ is the volume fraction of orientations in the element dg and that in the random case $f(g) = \text{const.} = 1$. This is fulfilled by introducing for the volume element *

$$dg = \frac{1}{8\pi^2} \sin \phi \, d\varphi_1 \, d\phi \, d\varphi_2 \quad (69)$$

$$\text{with} \quad \int f(g) dg = \int_0^{2\pi} \int_0^\pi \int_0^{2\pi} f(g) \frac{1}{8\pi^2} \sin \phi \, d\varphi_1 \, d\phi \, d\varphi_2 = 1 \quad (70)$$

$f(g)$ is commonly denoted as orientation distribution function (ODF). The density $P_{XYZ}(\alpha, \beta)$ of the poles $\{XYZ\}$ at the point α, β of the pole figure and the density $R_{s_i}(\gamma, \delta)$ of the sample axis s_i at the point γ, δ of the inverse pole figure can be obtained from the ODF by integration:

$$P_{XYZ}(\alpha, \beta) = \frac{1}{2\pi} \int_0^{2\pi} f(g) \, d\omega_{XYZ} \quad (71)$$

$$R_{s_i}(\gamma, \delta) = \frac{1}{2\pi} \int_0^{2\pi} f(g) \, d\omega_{s_i}. \quad (72)$$

Here is ω_{XYZ} and ω_{s_i} the angle of rotation around the axis $\{XYZ\}$ or s_i , respectively.

For representation of the ODF in the case of orthorhombic sample symmetry mostly the subregion H° (Eq. (67)) is used although this region generally contains each orientation 3 times. The use of the region has the advantage that it has no curved surfaces. The 3 subranges denoted as I, II and III which contain each orientation only once can be recognized in Fig. 14 and 16. In the radial cuts $\varphi_2 = \text{constant}$ (which are the radial cuts in Fig. 9), their boundaries appear as lines $\phi = \text{constant}$ which are shown in Fig. 17. It can be seen that best suited for studying the details of the orientation distribution is range I, since it is the largest range, since it is limited by only one curved surface and since it changes its dimension only little with changing φ_2 . For $\varphi_2 = 0^\circ$ and 90° it extends over $0 \leq \phi \leq 45^\circ$ and for $\varphi_2 = 45^\circ$ over $0 \leq \phi \leq 54,7^\circ$.

The ODF is commonly displayed by contour lines in sections $\varphi_2 = \text{const}$ or $\varphi_1 = \text{const}$. The sections are positioned mostly in distances of 5° from each other. Examples of ODF's displayed in this way are given by Fig. 17 ($\{236\}$ $\langle 385 \rangle$ texture) and Fig. 18 (cube texture $\{001\}$ $\langle 100 \rangle$). Both types of ODF's are observed as recrystallization texture of f.c.c. metals. Fig. 17 also demonstrates the appearance of a maximum of the ODF in the three basic regions of H° !

* This follows directly from the condition for the function $I(\varphi_1, \phi, \varphi_2)$

$$\iiint f(g) I \, d\varphi_1 \, d\phi \, d\varphi_2 = \iiint f(g g_0) I \, d\varphi_1 \, d\phi \, d\varphi_2$$

with g_0 being any rotation. Together with Eq. (70) this condition leads to $I = \sin \phi / 8\pi^2$.

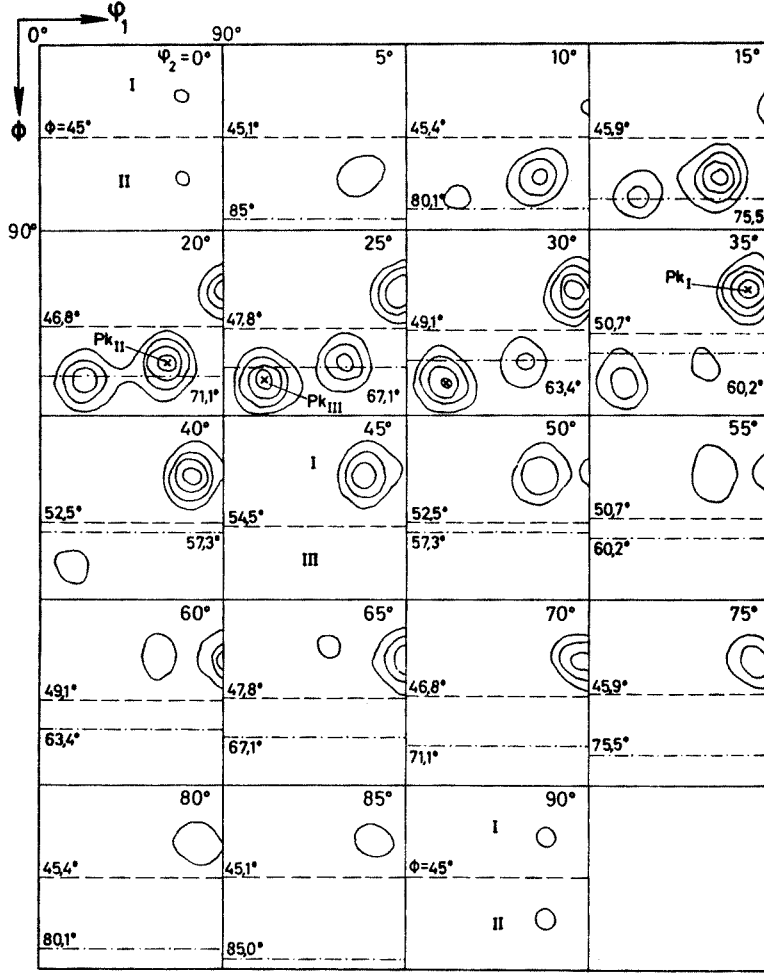


Fig. 17:
Presentation of an ODF consisting of a single component around the ideal orientation $\{236\} \langle 385 \rangle$ in the range H° of the Euler angle space. The orientation density is presented by contour lines in sections $\varphi_2 = \text{constant}$ taken at $\varphi_2 = 0^\circ, 5^\circ, 10^\circ$ etc. The maximum appears three times (Pk_I, Pk_{II}, Pk_{III}) corresponding to the three symmetrically equivalent subspaces indicated here by the dashed and dashed-dotted lines.

4.2 Distortion of the Euler Angle Space Near $\phi = 0$; Texture Components

Let us here consider the plane $\phi = 0$ of the Euler angle space. For the point $\varphi_1 = \phi = \varphi_2 = 0$ all three crystal axes $[001]$, $[010]$ and $[100]$ are parallel to the sample axes ND, TD and RD, i.e. this point describes the cube orientation $(001). [100]$. Since for $\phi = 0$ always sample coordinate ND and crystal coordinate are identical, the orientations in this plane are given by rotations of the cube orientations around ND.

In the plane $\phi = 0$ of the Euler angle space a peculiar degeneracy occurs. While, in general, an orientation is represented in the Euler angle space by a point, in the case $\phi = 0$ it is represented by a line. This follows from the matrix Eq. (19) which for $\phi = 0$ simplifies to

$$g(\varphi_1 \phi \varphi_2)_{\phi=0} = \begin{pmatrix} \cos(\varphi_1 + \varphi_2) & \sin(\varphi_1 + \varphi_2) & 0 \\ -\sin(\varphi_1 + \varphi_2) & \cos(\varphi_1 + \varphi_2) & 0 \\ 0 & 0 & 1 \end{pmatrix}. \quad (73)$$

One recognizes that in this plane an orientation is described not by one pair of angles φ_1, φ_2 , but by all pairs for which the sum $\varphi_1 + \varphi_2 = \text{constant}$, i.e. by -45° lines in the plane $\phi = 0$. This can be seen also directly from the definition of Euler angles. Since for $\phi = 0$ ND and $[001]$ are identical, the two rotations φ_1 and φ_2 can no longer be separated and only the total rotation $\varphi_1 + \varphi_2$ determines the orientation.

As example let us consider the cube orientation $\varphi_1 = \phi = \varphi_2 = 0$. By application of Eq. (19) one finds the symmetrically equivalent orientations which turn out to be the seven other corners of the cube of Fig. 16. Additionally, however, the cube orientation is also given by the -45° -lines in the plane $\phi = 0$ which are running through the cube corners situated in this plane, i.e. in particular by the line $\varphi_1 + \varphi_2 = \pi/2$ which runs between the corners $\varphi_2 = 0, \varphi_1 = \pi/2$ and $\varphi_2 = \pi/2, \varphi_1 = 0$. For this reason, the intensity along this line is always constant. This can be seen in Fig. 18 where a cube texture is shown. With increasing φ_2 , the maximum moves along the line $\phi = 0$ from $\varphi_1 = \pi/2$ to $\varphi_1 = 0$ without changing its height. In contrast to this, the symmetrically equivalent positions in the plane $\phi = \pi/2$ are not degenerated, i.e. with changing φ_2 the maxima situated at the corners at $\phi = 90^\circ$ do not shift but decrease in height, as also can be seen in Fig. 18.

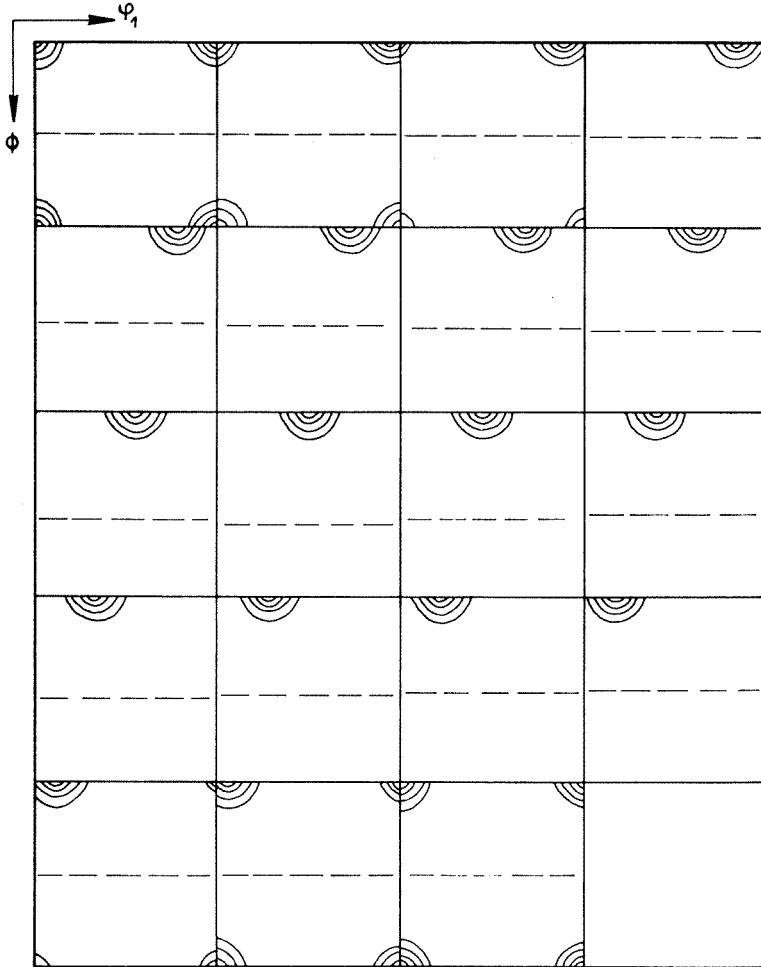


Fig. 18:
Presentation of the ODF of a
cube texture $\{001\} \langle 100 \rangle$ in the
manner described at Fig. 17.

Obviously such a degeneracy is obtained for all orientations in the plane $\phi = 0$, i.e. for those formed by rotation of the cube orientation around ND. E.g. for the orientation $(001) [110]$ one has $\varphi_1 + \varphi_2 = \pi/4$ which means that it is presented by all points on the -45° -line going from $\varphi_2 = 0, \varphi_1 = \pi/4$ to $\varphi_2 = \pi/4, \varphi_1 = 0$. (The other symmetrically equivalent orientations $\{001\} \langle 110 \rangle$ are given by the $\{\varphi_1 \phi \varphi_2\}$ -values $\{45, 90, 0\}$ and $\{45, 90, 90\}$).

This degeneracy at $\phi = 0$ is the reason for a strong distortion of the Euler angle space also for values $\phi \neq 0$. This can be seen best by considering all points in the Euler angle space which from a given point have a constant desorientation. (This is the smallest angle of rotation ω by which, independent of the axis of rotation, two orientations can be transformed into each other.) These points form a surface which, however, does not assume a shape of a sphere but, in the general case, a shape similar to that of an ellipsoide. Particularly in the plane $\phi = 0$ where an orientation is given by a -45° -line, one has only two other orientations with a given desorientation which form two lines parallel to the first one. At $\phi \neq 0$ an orientation is given again by a point, but this degeneracy still has the effect that for small values of ϕ ellipsoids are obtained which are strongly stretched out in the -45° direction.

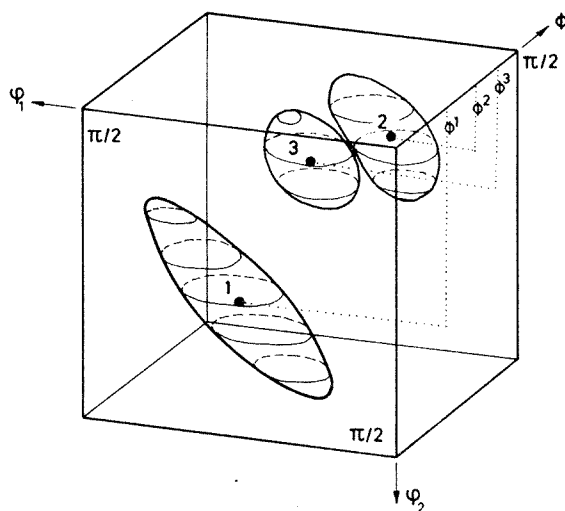


Fig. 19:
3-dimensional presentation of the three symmetrically equivalent components of the orientation $\{123\} \langle 634 \rangle$ in the range H_0 . The surfaces around the ideal orientation characterize a constant desorientation of 10° . The coordinates of the ideal orientations 1, 2 and 3 are $\{\varphi_1, \phi, \varphi_2\} = \{59.0, 36.7, 63.4\}$, $\{27.0, 57.7, 18.4\}$ and $\{52.9, 74.5, 33.7\}$, respectively.

Fig. 19 gives an example for the surfaces corresponding to a 10° desorientation from the three symmetrically equivalent orientations $\{123\} \langle 634 \rangle$. The ideal orientations 1, 2 and 3 are situated at $\phi = 36.7^\circ$, 57.7° and 74.5° , and one recognizes that the ellipsoids are stretched the more the smaller ϕ .

Often, in good approximation, the ODF can be considered as being superimposed by „isotropic components“, i.e. by orientation accumulations the density of which decreases from a maximum at an ideal orientation depending only of the desorientation (e.g. this accumulation may form of a three-dimensional Gauß type distribution in the desorientations /9, 10/). In such a case the contour lines correspond to surfaces of constant desorientation and thus have the same shape as above discussed for the ellipsoids. This shows up e.g. in Fig. 19 and also 17. It leads there to the fact that the maxima in the three symmetrically equivalent ranges of H° look very different although they represent the same orientation distribution.

The degeneracy in $\phi = 0$ is not the only reason for the deviation of the surfaces of constant desorientation from that of a sphere. For example the metric of the orientation space resulting in the factor $\sin \phi$ in Eq. (69) leads to a distortion in ϕ -direction. These questions, however, shall here not be discussed further.

4.3 Meaning of Special Lines and Planes in the Euler Angle Space

In order to be able to better visualize the orientation relationships occurring in the ODF, the meaning of some simple features of the Euler angle space should be kept in mind. For this purpose it is often useful to consider the cylindrical type of orientation space (Fig. 9).

The range H° is given there by the quadrant indicated by full lines. The sections $\varphi_2 = \text{const.}$ used in Figs. 17 and 18 appear here as radial sections parallel to the cylinder axis. With the definition of the Euler angles (Sec. 2.3) in mind, the meaning of some special lines and planes can immediately be realized.

It directly follows from the definition of the Euler angles that, with respect to the sample system S, the direction [001] is determined, only by the angles φ_1, ϕ . This means the lines parallel to the φ_2 -axis at fixed φ_1, ϕ indicate the different rotations around a fixed [001]-axis. For $\{\varphi_1, \phi\} = \{0 \text{ to } 90^\circ, 0\}$ this [001] axis is parallel to ND, for $\{0, 90^\circ\}$ parallel to TD and for $\{90^\circ, 90^\circ\}$ parallel to RD. (For $\phi = 0^\circ$, of course, the rotations are around [001] as well as ND.)

Vice versa, with respect to the crystal system C, the direction ND is determined only by the angles ϕ, φ_2 so that lines parallel to φ_1 at fixed ϕ, φ_2 indicate the rotations around a fixed ND. Since ND is given by the Miller indices {HKL}, these lines indicate also a rotation around a fixed crystallographic direction [HKL]. Here the values $\phi, \varphi_2 = \{0, 0 \text{ to } 90^\circ\}$ correspond to [HKL] = [001], $\{90^\circ, 0\}$ to [010], $\{90^\circ, 90^\circ\}$ to [100], $\{45^\circ, 0\}$ to [011], $\{54.7^\circ, 45^\circ\}$ to [111] etc. (c.f. Fig. 9). In Fig. 20 the lines for all values $\text{HKL} \leq 3$ are compiled and on these lines the orientations corresponding to values $\text{UVW} \leq 3$ are marked /11/.

One further recognizes that the lines running parallel the ϕ -axis at fixed φ_1, φ_2 indicate the different rotations around a fixed axis lying in the rolling plane forming the angle φ_1 to RD as well as in the plane {001} forming the angle φ_2 to [100]. Thus for $\varphi_1 = 0$ one has rotations around a fixed RD, for $\varphi_1 = 90^\circ$ around a fixed TD, for $\varphi_2 = 0$ around [100] and for $\varphi_2 = 90^\circ$ around [010]. If RD is given by the Miller indices [UVW], for $\varphi_1 = 0$ one has rotations around the crystallographic axis [UVW] (which is determined by φ_2). The line determined by the values $\{\varphi_1, \varphi_2\} = \{0, 0\}$ corresponds to rotations of the cube orientation around RD or [100], $\{0, 90^\circ\}$ to such around RD or $[0 \bar{1} 0]$, $\{90^\circ, 0\}$ to such around TD or $[1 0 0]$ and $\{90^\circ, 90^\circ\}$ to such around TD or $[0 \bar{1} 0]$.

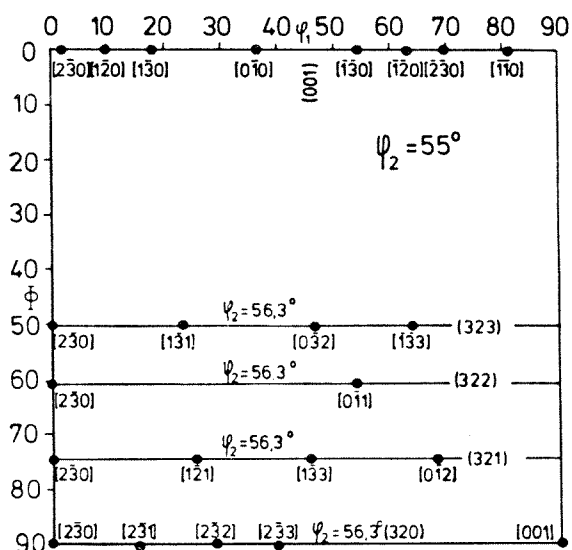
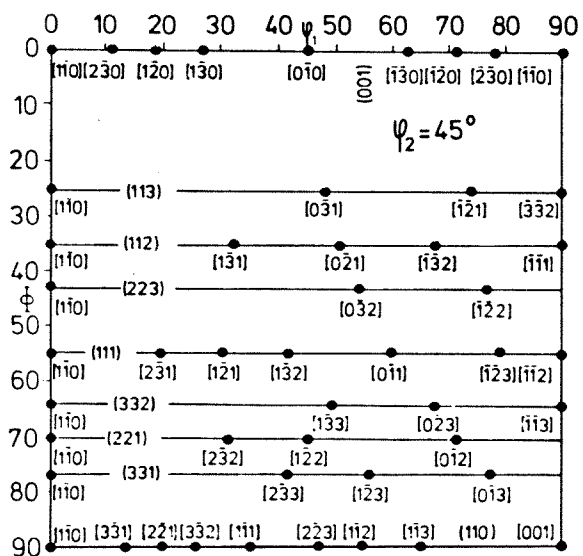
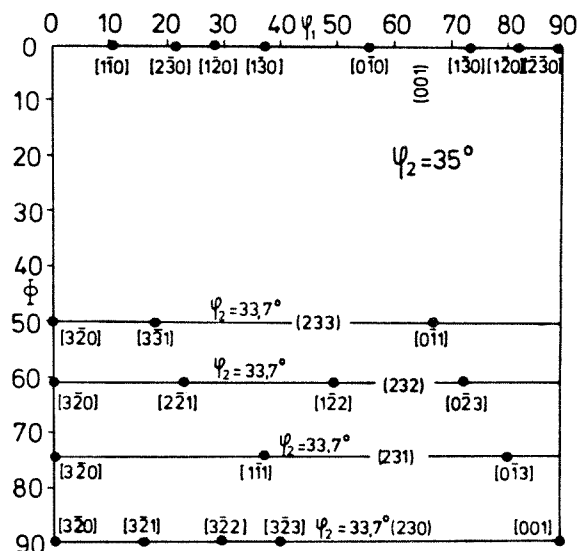
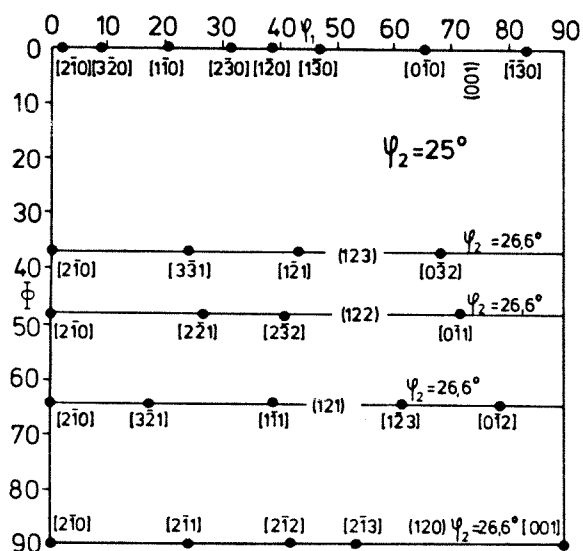
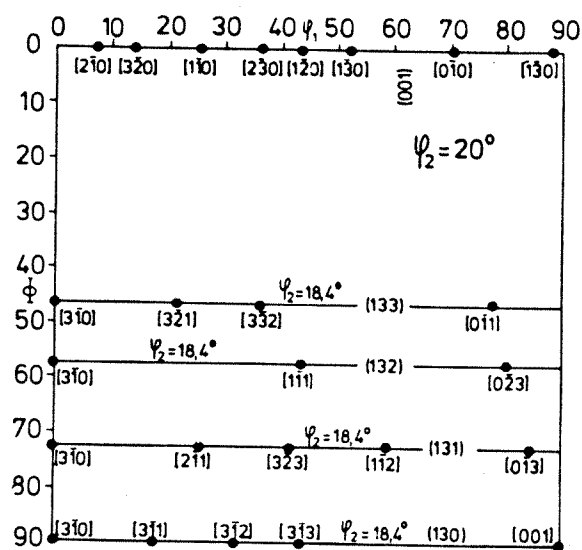
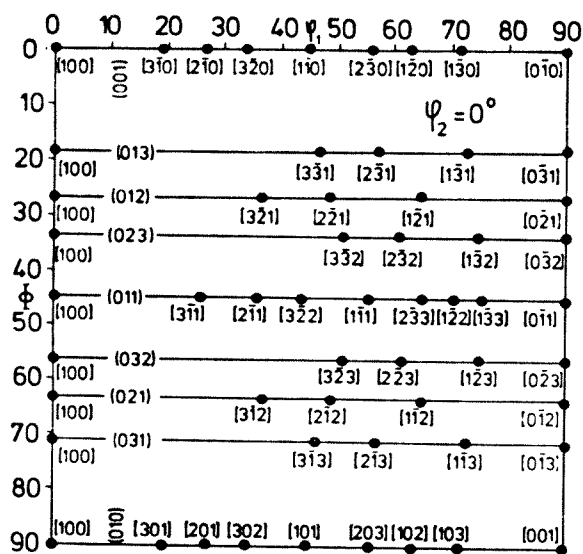
4.4 The Multiplicity of Orientations

The fact that, due to symmetry of crystal and sample, a given orientation possesses symmetrically equivalent orientations in the asymmetric unit H of the Euler angle space (Eq. (55), Fig. 8) is denoted as „multiplicity” of this orientation. As shown above, in the case of cubic crystal and orthorhombic sample symmetry this multiplicity is 96. This, however, is correct only for a general orientation. If by symmetry elements of the sample a certain orientation is transformed within itself, some (in general i) of these equivalent positions fall together so that for such a special orientation the multiplicity is reduced to $96/i$.

In the here mainly considered case of cubic/orthorhombic specimen/sample symmetry, always two symmetrically equivalent orientations fall together if they are situated on the rotation axes $L_{\varphi_1}^2$ or $L_{\varphi_2}^2$, the mirror plane P_ϕ , the mirror lines L^M or the mirror points L^P . As can be seen from Fig. 16 and from Table 3.5 where these symmetry elements are listed, all these special orientations are characterized by a $\langle 100 \rangle$ or $\langle 110 \rangle$ -axis lying either in ND, TD or RD. This means that the multiplicity is reduced to $96/2 = 48$ for all orientations for which one of the 3 sets of Miller indices {HKL}, {UVW} or {QRS} is given by $\langle 100 \rangle$ or $\langle 110 \rangle$.

In the intersection points of two of these symmetry elements the multiplicity is reduced again by a factor of 2 resulting in a multiplicity of 24. This is the case also for the mirror points on the edges parallel to φ_1 of the cube (Fig. 16), since, at the same time, these points lie on a mirror plane for $\phi = 0$ or on a two-fold axis (for $\phi = 90^\circ$). (The mirror points on the line Q^3 , also the ones being situated on two-fold axes, have only the multiplicity 48, since along the line Q^3 the symmetry operations of the mirror points and these axes are identical.) As can be seen in Fig. 20, these points with a multiplicity of 24 are the orientations $\{001\} \langle 100 \rangle \langle 100 \rangle$, $\{001\} \langle 110 \rangle \langle 110 \rangle$, $\{011\} \langle 100 \rangle \langle 110 \rangle$ and $\{011\} \langle 110 \rangle \langle 100 \rangle$. (It is not possible to have only two of the sets {HKL}, {UVW} or {QRS} given by $\langle 100 \rangle$ or $\langle 110 \rangle$.)

The multiplicity is rather important for the interpretation of textures. For example, let us consider a texture consisting of „components” in form of pronounced maxima of the ODF. Supposing that their volume fraction and scattering width would be equal, a maximum situated at such a special orientation would possess i times the height of a maximum situated at a general orientation. In such a case i different



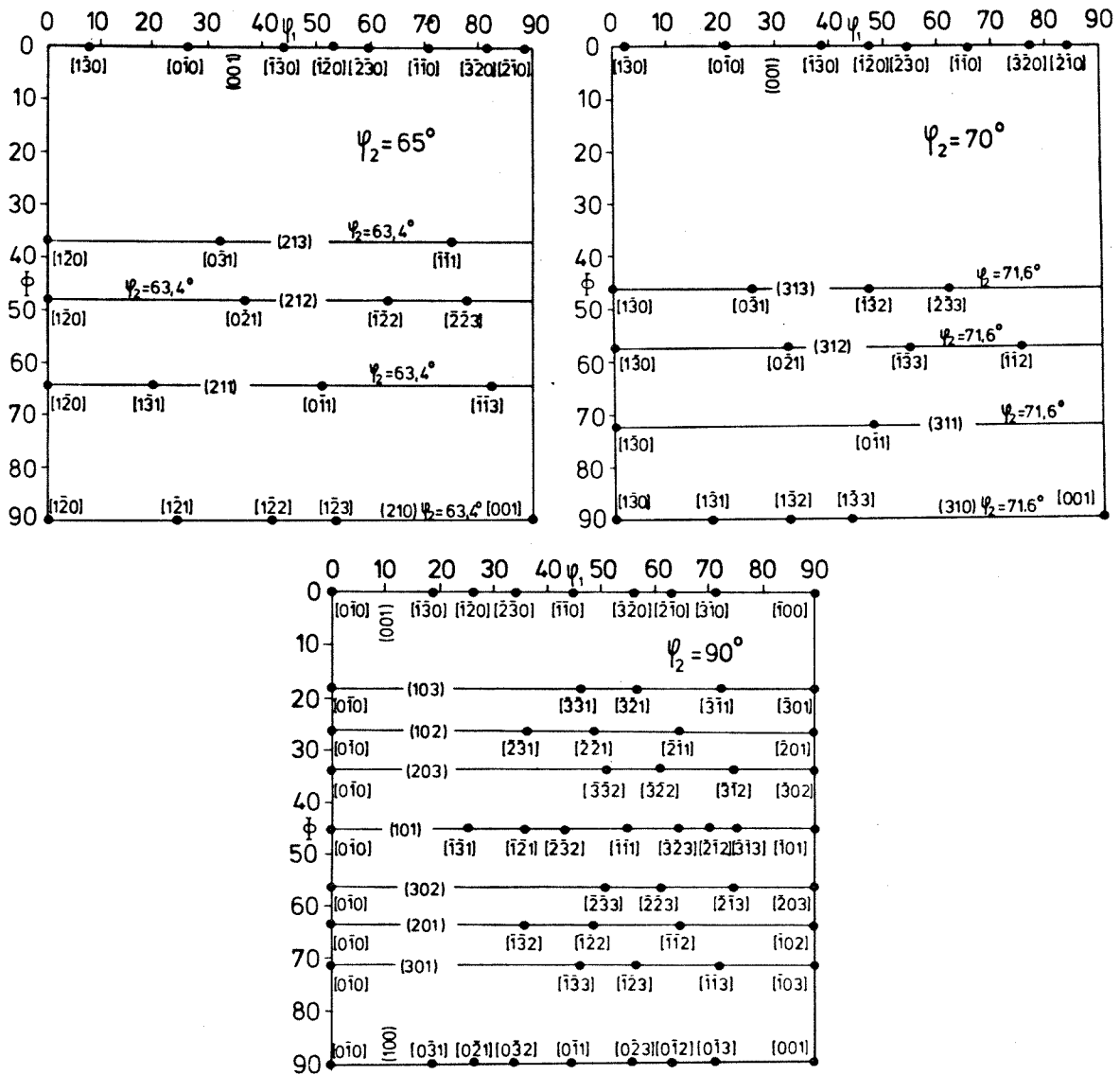


Fig. 20:
Positions of the orientations (HKL) [UVW] with $|H, K, L, U, V, W| \leq 3$ in sections $\varphi_2 = \text{constant}$ through the range H° of the Euler angle space. In the case that the φ_2 -value of such an orientation does not exactly coincide with that of the φ_2 -values of the selected sections, the points are inserted in the section with a φ_2 -value closest to the exact one.

maxima which, in the general case, would occur at i different positions (not necessarily all of them inside H°) will fall on top of each other. Fig. 17 gives an example of a position of the multiplicity of 96 ($\{236\} \langle 385 \rangle$) and Fig. 18 of the multiplicity of only 24 (cube positions $\{001\} \langle 100 \rangle$).

In the case of cubic single crystals one has triclinic sample symmetry and thus the multiplicity 24. In this case no special orientations with reduced multiplicity exist. (The symmetry elements are either translations or screw axes, i.e. elements which do not transform points into themselves.) At monoclinic sample symmetry the multiplicity is 48 in the general case, but can be reduced to 24 for special orientations.

4.5 The ODF in Equivalent Regions

As pointed out above, for representing the ODF in the Euler angle space for samples with triclinic, monoclinic or orthorhombic symmetry the ranges H' , H'' or H° , respectively, have to be applied. They contain each orientation three times. Sometimes, however, it is useful to consider the ODF also outside these basic ranges. These values can be obtained from the values inside by transformations which directly follow from the symmetry relationships listed in Table 3.5.

In Fig. 21 (for the triclinic and monoclinic case) and in Fig. 22 (for the orthorhombic case) this is demonstrated for the ranges neighbouring the above basic ranges by inserting the expressions which give the transformation from each of these ranges into the basic range. The parts of the Euler angle space further away from the basic ranges can be transformed into the range shown in Figs. 21 and 22 a) by making use of the identical equivalency due to the periodicity in $2/\pi$ of the Euler angles $\varphi_1 \phi \varphi_2$.

4.6 Orientation Transformations and Orientation Relationships

For orientation transformation mostly the rotation parameters \vec{v} , ω are used. If the orientation g is transformed by a rotation around an axis connected with the crystal, the new orientation g' is given by

$$g' = g(\vec{v}, \omega) \cdot g. \quad (74)$$

Transformation with respect to an axis connected with the specimen yields an orientation g'' given by

$$g'' = g \cdot g(\vec{v}, \omega). \quad (75)$$

For example, if one inserts $v_x = 1$, $v_y = v_z = 0$ into the matrix (29) and introduces this matrix into Eq. (74) or (75), g' and g'' represent orientations obtained from g by rotation by the angle ω around $[100]$ or RD, respectively.

Rotations with respect to a crystal axis are found, for example, at martensitic transformations or at twinning. For twinning in f.c.c. crystals one has to introduce $\vec{v} = \langle 111 \rangle$, $\omega = 180^\circ$ and for b.c.c. metals $\vec{v} = \langle 112 \rangle$, $\omega = 180^\circ$. In Table 4.6 for the resulting orientation relationships are compiled. An example for rotations around a sample axis is the texture change during rolling where often rotations around TD or RD are observed.

Another application makes use of the transformation

$$g(\vec{v}', \omega) = h \cdot g(\vec{v}, \omega) \cdot h^{-1}. \quad (76)$$

With h being any rotation matrix, this operation describes a transformation which does not change the trace of the matrix g , i.e. the sum $g_{11} + g_{22} + g_{33}$. This means that this transformation alters only the axis of rotation (from \vec{v} to \vec{v}') but not the angle ω (Eq. (29)). If h is a symmetry element, then \vec{v}' means an axis of rotation symmetrically equivalent to \vec{v} , and, correspondingly, $g(\vec{v}', \omega)$ a transformation symmetrically equivalent to $g(\vec{v}, \omega)$. If, for example, $g(\vec{v}, \omega)$ describes the Kurdjumov-Sachs relationship $90^\circ [11\bar{2}]$, then the 90° rotations around all other $\langle 112 \rangle$ -axis are obtained simply by applying for h the cubic symmetry elements given in Table 3.2.

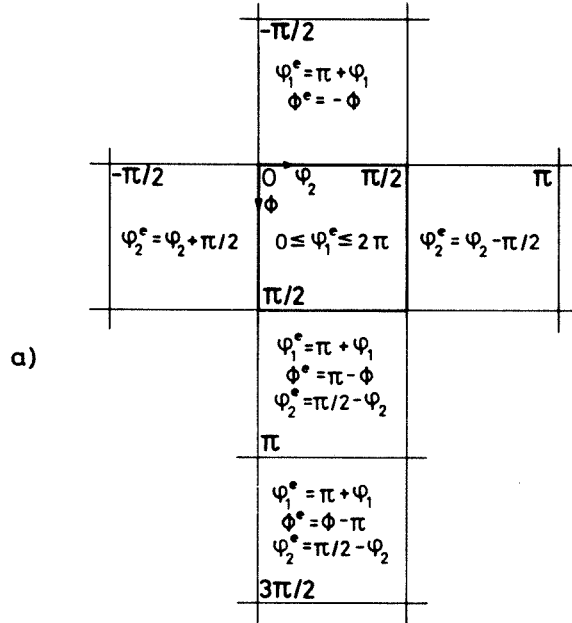


Fig. 21:
Transformations leading from different parts of the Euler angle space into the basic range H' for the triclinic case or into the range H'' for the monoclinic case. In case that two different sets of expressions are listed, the ones in parenthesis are valid for the monoclinic case.

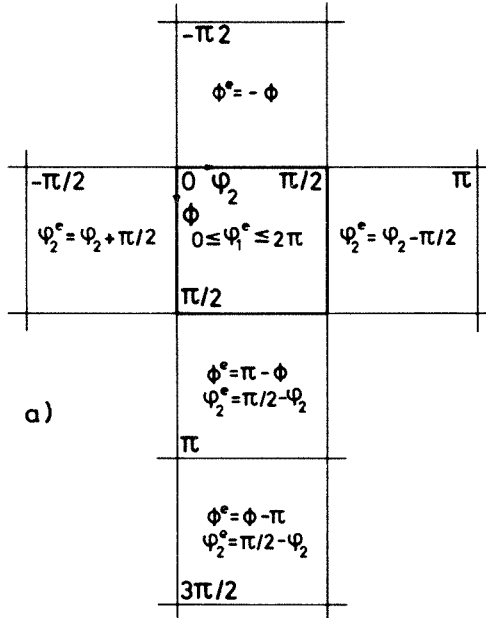
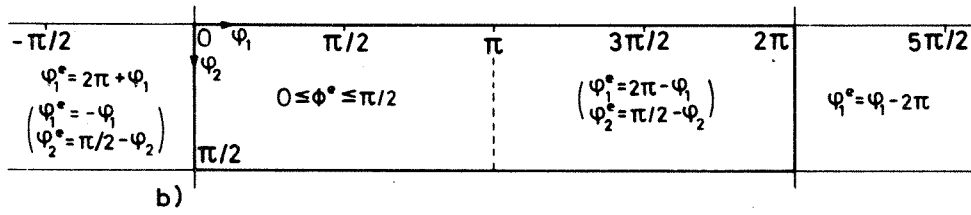


Fig. 22:
Transformations leading from different parts of the Euler angle space into the basic range H'' for the orthorhombic case.

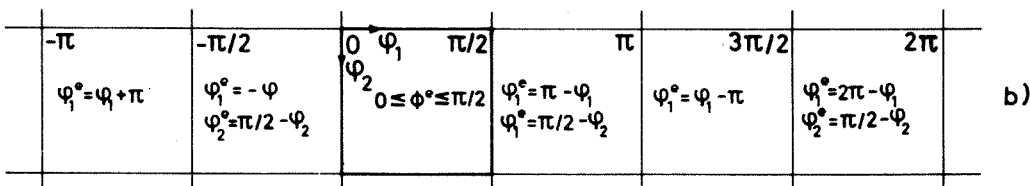


Table 4.6: The Millers indices ($H'K'L'$) [$U'V'W'$] for the four $\{111\}$ -twins and the twelve $\{112\}$ -twins of a given orientation (HKL) [UVW]

111	$\bar{1}\bar{1}1$	$1\bar{1}\bar{1}$	$\bar{1}\bar{1}\bar{1}$
H' - $H + 2K + 2L$	- $H - 2K - 2L$	- $H - 2K + 2L$	- $H + 2K - 2L$
K' $2H - K + 2L$	- $2H - K + 2L$	- $2H - K - 2L$	$2H - K - 2L$
L' $2H + 2K - L$	- $2H + 2K - L$	$2H - 2K - L$	- $2H - 2K - L$
U' - $U + 2V + 2W$	- $U - 2V - 2W$	- $U - 2V + 2W$	- $U + 2V - 2W$
V' $2U - V + 2W$	- $2U - V + 2W$	- $2U - V - 2W$	$2U - V - 2W$
W' $2U + 2V - W$	- $2U + 2V - W$	$2U - 2V - W$	- $2U - 2V - W$
112	$\bar{1}\bar{1}2$	$1\bar{1}\bar{2}$	$\bar{1}\bar{1}\bar{2}$
H' - $2H + K + 2L$	- $2H - K - 2L$	- $2H - K + 2L$	- $2H + K - 2L$
K' $H - 2K + 2L$	- $H - 2K + 2L$	- $H - 2K - 2L$	$H - 2K - 2L$
L' $2H + 2K + L$	- $2H + 2K + L$	$2H - 2K + L$	- $2H - 2K + L$
U' - $2U + V + 2W$	- $2U - V - 2W$	- $2U - V + 2W$	- $2U + V - 2W$
V' $U - 2V + 2W$	- $U - 2V + 2W$	- $U - 2V - 2W$	$U - 2V - 2W$
W' $2W + 2V + W$	- $2U + 2V + W$	$2U - 2V + W$	- $2U - 2V + W$
121	$\bar{1}2\bar{1}$	$1\bar{2}\bar{1}$	$\bar{1}\bar{2}\bar{1}$
H' - $2H + 2K + L$	- $2H - 2K - L$	- $2H - 2K + L$	- $2H + 2K - L$
K' $2H + K + 2L$	- $2H + K + 2L$	- $2H + K - 2L$	$2H + K - 2L$
L' $H + 2K - 2L$	- $H + 2K - 2L$	- $H - 2K - 2L$	- $H - 2K - 2L$
U' - $2U + 2V + W$	- $2U - 2V - W$	- $2U - 2V + W$	- $2U + 2V - W$
V' $2U + V + 2W$	- $2U + V + 2W$	- $2U + V - 2W$	$2U + V - 2W$
W' $U + 2V - 2W$	- $U + 2V - 2W$	- $U - 2V - 2W$	- $U - 2V - 2W$
211	$\bar{2}1\bar{1}$	$2\bar{1}\bar{1}$	$\bar{2}\bar{1}\bar{1}$
H' $H + 2K + 2L$	$H - 2K - 2L$	$H - 2K + 2L$	$H + 2K - 2L$
K' $2H - 2K + L$	- $2H - 2K + L$	- $2H - 2K - L$	$2H - 2K - L$
L' $2H + K - 2L$	- $2H + K - 2L$	$2H - K - 2L$	- $2H - K - 2L$
U' $U + 2V + 2W$	$U - 2V - 2W$	$U - 2V + 2W$	$U + 2V - 2W$
V' $2U - 2V + W$	- $2U - 2V + W$	- $2U - 2V - W$	$2U - 2V - W$
W' $2U + V - 2W$	- $2U + V - 2W$	$2U - V - 2W$	- $2U - V - 2W$

Table 4.6: The Millers indices ($H'K'L'$) [$U'V'W'$] for the four $\{111\}$ -twins and the twelve $\{112\}$ -twins of a given orientation (HKL) [UVW]

111	$\bar{1}\bar{1}1$	$1\bar{1}\bar{1}$	$\bar{1}\bar{1}\bar{1}$
H' - $H + 2K + 2L$	- $H - 2K - 2L$	- $H - 2K + 2L$	- $H + 2K - 2L$
K' $2H - K + 2L$	- $2H - K + 2L$	- $2H - K - 2L$	$2H - K - 2L$
L' $2H + 2K - L$	- $2H + 2K - L$	$2H - 2K - L$	- $2H - 2K - L$
U' - $U + 2V + 2W$	- $U - 2V - 2W$	- $U - 2V + 2W$	- $U + 2V - 2W$
V' $2U - V + 2W$	- $2U - V + 2W$	- $2U - V - 2W$	$2U - V - 2W$
W' $2U + 2V - W$	- $2U + 2V - W$	$2U - 2V - W$	- $2U - 2V - W$
112	$\bar{1}\bar{1}2$	$1\bar{1}\bar{2}$	$\bar{1}\bar{1}\bar{2}$
H' - $2H + K + 2L$	- $2H - K - 2L$	- $2H - K + 2L$	- $2H + K - 2L$
K' $H - 2K + 2L$	- $H - 2K + 2L$	- $H - 2K - 2L$	$H - 2K - 2L$
L' $2H + 2K + L$	- $2H + 2K + L$	$2H - 2K + L$	- $2H - 2K + L$
U' - $2U + V + 2W$	- $2U - V - 2W$	- $2U - V + 2W$	- $2U + V - 2W$
V' $U - 2V + 2W$	- $U - 2V + 2W$	- $U - 2V - 2W$	$U - 2V - 2W$
W' $2W + 2V + W$	- $2U + 2V + W$	$2U - 2V + W$	- $2U - 2V + W$
121	$\bar{1}2\bar{1}$	$1\bar{2}\bar{1}$	$\bar{1}\bar{2}\bar{1}$
H' - $2H + 2K + L$	- $2H - 2K - L$	- $2H - 2K + L$	- $2H + 2K - L$
K' $2H + K + 2L$	- $2H + K + 2L$	- $2H + K - 2L$	$2H + K - 2L$
L' $H + 2K - 2L$	- $H + 2K - 2L$	- $H - 2K - 2L$	- $H - 2K - 2L$
U' - $2U + 2V + W$	- $2U - 2V - W$	- $2U - 2V + W$	- $2U + 2V - W$
V' $2U + V + 2W$	- $2U + V + 2W$	- $2U + V - 2W$	$2U + V - 2W$
W' $U + 2V - 2W$	- $U + 2V - 2W$	- $U - 2V - 2W$	- $U - 2V - 2W$
211	$\bar{2}1\bar{1}$	$2\bar{1}\bar{1}$	$\bar{2}\bar{1}\bar{1}$
H' $H + 2K + 2L$	$H - 2K - 2L$	$H - 2K + 2L$	$H + 2K - 2L$
K' $2H - 2K + L$	- $2H - 2K + L$	- $2H - 2K - L$	$2H - 2K - L$
L' $2H + K - 2L$	- $2H + K - 2L$	$2H - K - 2L$	- $2H - K - 2L$
U' $U + 2V + 2W$	$U - 2V - 2W$	$U - 2V + 2W$	$U + 2V - 2W$
V' $2U - 2V + W$	- $2U - 2V + W$	- $2U - 2V - W$	$2U - 2V - W$
W' $2U + V - 2W$	- $2U + V - 2W$	$2U - V - 2W$	- $2U - V - 2W$

APPENDIX

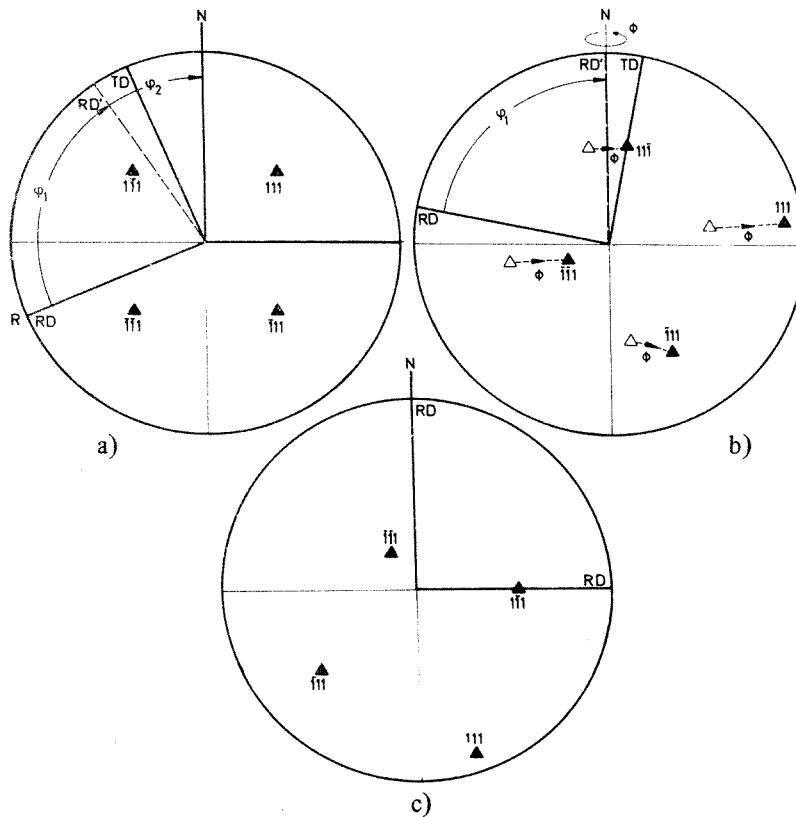
GRAPHICAL CONSTRUCTION OF A POLE FIGURE FROM EULER ANGLES

As shown in Sec. 2.3 the Euler angles transform the sample system S into the crystal system C by a sequence of three independent rotations. These rotations can easily be carried out graphically in such a way that only by the usual application of Wulff net (and a sheet of transparent paper) a pole figure is obtained. The idea of the method is to exchange the sequence of the partial rotations in the total rotation

$$g(\varphi_1 \phi \varphi_2) = g(\varphi_2) \cdot g(\phi) \cdot g(\varphi_1)$$

and correct this by the proper choice of the rotation axes.

First the direction RD will be laid in the direction N („north”) of the Wulff net. Then, by a rotation by $(\varphi_1 + \varphi_2)$ around the center, RD is brought into the direction R (Fig. 23 a) and the poles in question (in Fig. 23 a the $\{111\}$ -poles) are drawn into the sheet in standard position with respect to the original position (filled symbols in Fig. 23 a). Now by a reversed rotation by φ_2 a sample axis RD' is brought into N, and, by this rotation, the poles (here $\{111\}$) are taken into a new position (open symbols in Fig. 23 b). Subsequently by a rotation by ϕ around $N = RD'$ the poles are shifted again (into the filled symbols of Fig. 23 b). Finally by reversed rotation by φ_1 , RD is brought back into N and thus the poles into their final positions (filled symbols in Fig. 23 c).



REFERENCES

- /1/ H.J. Bunge, *Mathematische Methoden der Texturanalyse*, Akademie-Verlag, Berlin 1961.
- /2/ *Proceedings of the Internal Seminar*, Cracow 1971.
- /3/ J. Jura, J. Pospiech, H.J. Bunge, *Papers of Commission of Metallurgy and Foundry, Metalurgia* 24 (1976), 111.
- /4/ R.J. Roe, *Journ. Appl. Phys.* 36 (1965), 2024.
- /5/ J. Pospiech, *Kristall u. Technik* 7 (1972), 1074.
- /6/ G. Ibe, K. Lücke, *Texture* 1 (1972), 87.
- /7/ J. Pospiech, A. Gnatek, K. Fichtner, *Kristall u. Technik* 9 (1974), 729.
- /8/ I.M. Gelfand, R.A. Minlos, Z.YA. Shapiro, *Representations of the Rotation and Lorentz Groups and their Applications*, Pergamon Press, Oxford—London—New York—Paris 1963.
- /9/ W. Truszkowski, J. Pospiech, J. Jura, B. Major, 3^e colloque européen sur les textures de déformation et de recristallisation des métaux et leurs applications industrielles, Pont-à-Mousson 1973.
- /10/ K.H. Virnich, J. Pospiech, A. Flemmer, K. Lücke, (paper 1.1); K.H. Virnich, K. Lücke, (paper 5.2); K.H. Virnich, G. Köhlhoff, K. Lücke, J. Pospiech, (paper 5.9); *Proceedings of the fifth International Conference of Textures of Materials*, Springer-Verlag, Berlin—Heidelberg—New York, in press.
- /11/ D. Schläfer, H.J. Bunge, VII Konferencja Naukowa-Techniczna, Gliwice 1974.

7.4. COREC

```

SUBROUTINE COREC
DIMENSION T(19,19),TG(19),TR(19)
COMMON FEY(17,18,4),R(19,19)
COMMON /SET/ IN,INP,LIB,IOUT,LTP,LMB
COMMON /DAT/ HEAD(22),ACT(10)
COMMON /PAR/ LMAX,LFMAX
COMMON /ORG/ LIFI,LOK,J1,13
DATA XCOR/3HCOR/
DATA XT/1PT/,XR/1HR/
800 CONTINUE
READ(INP,1004)HKL,DF,DFM
HEAD(LOK+1)=HKL
HEAD(LOK+2)=DF
HEAD(LOK+3)=DFM
WRITE(IOUT,3100) HKL
READ(INP,1900) COR,SR
WRITE(IOUT,3200) COR,SR
IF(COR.EQ.XCOR) GO TO 664
GO TO 555
664 CONTINUE
READ(INP,1004)GP,GT
WRITE(IOUT,3300) GP,GT
WRITE(IOUT,3500) DF,DFM
J1=INT(90.00001/DF)+1
I1=INT((GP+.0001)/DF)+1
I2=INT((GT+.0001)/DF)+1
I3=INT(90.00001/DF)+1
IF(I2-I1)665,665,666
665 CONTINUE
ISTR=3
IF(SR.EQ.XT)ISTR=1
IF(SR.EQ.XR)ISTR=2
READ(INP,1006)(TR(K),K=1,I1)
WRITE(IOUT,4001)
WRITE(IOUT,2000)(TR(K),K=1,I1)
READ(INP,1006)(TG(K),K=12,I3)
WRITE(IOUT,4002)
WRITE(IOUT,2000)(TG(K),K=12,I3)
WRITE(IOUT,4003)
K0=1
DO 11 K=K0,I1
READ(INP,1006)(R(KK,K),KK=1,J1)
WRITE(IOUT,2000)(R(KK,K),KK=1,J1)
11 CONTINUE
DO 121 K=1,I1
DO 121 KK=1,J1
121 R(KK,K)=R(KK,K)*TP(K)
WRITE(IOUT,4004)
DO 12 K=12,I3
READ(INP,1006)(T(KK,K),KK=1,J1)
WRITE(IOUT,2000)(T(KK,K),KK=1,J1)
12 CONTINUE
DO 13 K=12,I3
DO 13 KK=1,J1
13 T(KK,K)=T(KK,K)*TG(K)
X=0.
Y=0.
DO 14 K=12,I1
DO 14 KK=1,J1

```

```

4003 FORMAT(1H ///11H MATRIX R//)
4004 FORMAT(1H ///11H MATRIX T //)
END

```

7.2. TWODIM

```

SUBROUTINE TWODIM
DIMENSION DESCR(19)
DIMENSION NOR(18)
DIMENSION D(18,20),P(20),A(40)
COMMON FEY(17,18,4),R(19,19)
COMMON /SET/ IN,INP,LIB,IOUT,LTP,LMB
COMMON /DAT/ HEAD(22),ACT(10)
COMMON /PAR/ LMAX,LFMAX
COMMON /ORG/ LIFI,LOK,J,I
DATA NOR/1,2,3,4,5,6,7,8,9,10,11,12,13,14,15,16,17,18/
EQUIVALENCE (LMAX,L)
EQUIVALENCE (IOUT,LUO)
XB=0.017453293
DF=HEAD(LOK+1)
DFM=HEAD(LOK)
JP1=J
IP1=I
DO 750 JX=1,JP1
750 DESCR(JX)=DFM*FLOAT(JX=1)
DO 8 IM=1,IP1
Y=SIN(FLOAT(IM=1)*DF*XB)
DO 9 JM=1,JP1
P(JM)=R(JM,IM)*Y
P(JP1)=0.5*P(JP1)
LP1=L+1
DO 10 N=1,LP1
X=0.5*P(1)
XNN=FLOAT(N=1)*DFM*XB*2.0
DO 11 JM=2,JP1
11 X=X+COS(FLOAT(JM=1)*XNN)*P(JM)
D(N,IM)=X
10 CONTINUE
8 CONTINUE
DO 12 N=1,LP1
12 D(N,IP1)=0.5*D(N,IP1)
X=D(1,1)
DO 13 IM=2,IP1
13 X=X+D(1,IM)
Y=12.5663706/(8.0*X*DF*DFM*XB*XB)
DO 201 L2=1,I
DO 201 L22=1,J
201 R(L22,L20)=R(L22,L20)*Y
XX=X
WRITE(LUO,1004)Y
WRITE(LUO,2201) HEAD(LOK+2)
WRITE(LUO,3030)(DESCR(JX),JX=1,JP1)
DO 20 L20=1,I
XYZ=DF*FLOAT(L20=1)
20 WRITE(LUO,2020) XYZ,(R(L22,L20),L22=1,J)
LN1=L+1
WRITE(LUO,1005)(NOR(K),K=1,LN1)
ISRD=2
IF(DF.EQ.5.) ISRD=1
IF(ISRD.EQ.1) GO TO 710
DO 711 I=1,188
711 PFAD(LIB)

```

```

      X=X+R(KK,K)*T(KK,K)
      GOTO(142,141,555)ISTR
142  Y=Y+T(KK,K)**2
      GOTO 14
141  CONTINUE
      Y=Y+R(KK,K)**2
14   CONTINUE
      XNORM=X/Y
      WRITE(IOUT,1007) XNORM
      X=0.
      DO 15 K=1,J1
15   X=X+R(K,1)
      Y=X/FLOAT(J1)
      DO 16 K=1,J1
16   R(K,1)=Y
      GOTO(162,161) ISTR
161  CONTINUE
      KK=I2-1
      DO 17 K=1,KK
      DO 17 KA=1,J1
17   R(KA,K)=R(KA,K)*XNORM
      DO 18 K=I2,I3
      DO 18 KK=1,J1
18   R(KK,K)=T(KK,K)
      GOTO 19
162  KK=I1+1
      DO 181 K=KK,I3
      DO 181 KA=1,J1
181  R(KA,K)=T(KA,K)*XNORM
19   CONTINUE
      WRITE(IOUT,2010) HKL
      DO 70 LAY=1,I3
70   WRITE(IOUT,2001)(R(LAX,LAY),LAX=1,J1)
      GO TO 876
555  WRITE(IOUT,1555)
      PAUSE 555
      GO TO 800
666  WRITE(IOUT,3000)
      PAUSE 666
      GO TO 800
876  CONTINUE
      LOK=LOK+3
      RETURN
1004 FORMAT(3F10.0)
1006 FORMAT(8F10.2)
1007 FORMAT(1H //48H  NORMALISATION FROM *CORRECTION* PROGRAM NC=
      *,F13.6//)
1555 FORMAT(46H  WRONG OR MISSING CONTROL CARD FOR CORRECTION)
1900 FORMAT(A3,A1)
2000 FORMAT(1H /(8F13.3))
2001 FORMAT(1H //(8F13.3))
2010 FORMAT(1H1////41H  CORRECTED MATRIX P FOR FIGURE  HKL= ,F5.0//
      */)
3000 FORMAT(33H  MATRIX R AND T NOT COINCIDE)
3100 FORMAT(1H1////38X,38H  EVIDENCE  FOR  POLE  FIGURE  HKL=,F5.0//
      */)
3200 FORMAT(1H ,25H  TYPE OF CORRECTION  ,A3,2X,A1//)
3300 FORMAT(1H ,26H  ANGULAR LIMITS  FR=,F6.1,7H  GT=,F6.1//)
3500 FORMAT(1H ,26H  ANGULAR INTERVALS  RAD=,F6.1,7H  NORM=,F6.1//)
4001 FORMAT(1H //26H  CORRECTIONS FOR MATRIX R//)
4002 FORMAT(1H //26H  CORRECTIONS FOR MATRIX T//)

```

```

710  CONTINUE
      DO 14 LM=1,L
      L*P1=LM+1
      DO 15 N=1,LMP1
      IF(ISRD,EQ.2) GO TO 713
      READ(LIB) A
      Y=0.0
      DO 16 IM=1,IP1
      Y=Y+A(IM)*D(N,IM)
16   CONTINUE
      GO TO 714
713  PFAD(LIB) A
      Y=0.0
      DO 715 IM=1,IP1
      X=A(1)
      XII=FLOAT(IM-1)*DF*XB*2.
      DO 17 IS=2,LMP1
17   X=X+A(IS)*COS(FLOAT(IS-1)*XII)
      Y=Y+X*D(N,IM)
715  CONTINUE
714  CONTINUE
      Y=Y*7.0898154/XX
      IF(N,NE.1) GO TO 18
      Y=Y*0.70710678
18   CONTINUE
      FEX(LM,N,LIFI)=Y
15   CONTINUE
14   CONTINUE
      REWIND LIB
      DO 30 LM=1,L
      LT2=2*LM
      LMP1=LM+1
30   WRITE(LU0,2030) LT2,(FEX(LM,N,LIFI),N=1,LMP1)
      RETURN
1004 FORMAT(1H1////46H  TWO DIMENSIONAL ANALYSIS NORMALISATION NI=,
      *F13.6//)
1005 FORMAT(1H1////24H  MATRIX F EXPERIMENTAL ///1H ,10X,10I10/1H ,10X
      *,10I10)
2020 FORMAT(1H /(20F6.1//)
2201 FORMAT(1H ///31H  NORMALIZED POLE FIGURE HKL = ,F5.0//)
2030 FORMAT(1H /1H ,I10,10F10.4/1H ,10X,10F10.4)
3030 FORMAT(1H /6X,(19F6.1))
      END

```

7.3. COEF

```

SUBROUTINE COEF
  DIMENSION XK(16,3,8),B(3,18),F1(18,4),DFA(18),DC(18,3),C(16,3,18)
  DIMENSION AA(3,3),AQ(3,3),NRH(4),MODHKL(8),M(17)
  DIMENSION NOR(18)
  COMMON FEX(17,18,4),R(19,19)
  COMMON /SET/ IN,INP,LIB,IOUT,LTP,LMB
  COMMON /DAT/ HEAD(22),ACT(10)
  COMMON /PAR/ LMAX,LMAX
  COMMON /ORG/ LIFI,LOK,J,I
  DATA PI/12.56637/
  DATA NOR/1,2,3,4,5,6,7,8,9,10,11,12,13,14,15,16,17,18/
  DATA MODHKL/100,110,111,102,112,122,103,113/
  DATA M/0,1,1,1,1,2,1,2,2,2,3,2,3,3,3,3/
  EQUIVALENCE (LMAX,L)
  EQUIVALENCE (IOUT,LOUT)

```

```

C
DO 99 K=1,170
99 READ(LIB)
   READ(LIB) XK
   REWIND LIB

C
WRITE(LOUT,7000)
LIFI=LFMAX
LOKX=LOK
DO 4 K=1,LIFI
  K1=LIFI-K+1
  LOKX=LOKX-3
  NHK=INT(HEAD(LOKX+1))
  DO 5 K2=1,8
    IF(MODHKL(K2),EQ,NHK) GOTO 6
5 CONTINUE
6 NRH(K1)=K2
4 CONTINUE
  Z=1.0
  DO 10 LM=2,L
    LMP1=LM+1
    LMN1=LM-1
    LTL=M(LM)
    U=PI/(FLOAT(LM)*4.+1.)
    DO 11 LT=1,LTL
      DO 12 M1=1,LTL
        X=0.
        DO 13 IH=1,LIFI
          KH=NRH(IH)
13 X=X+XK(LMN1,LT,KH)*XK(LMN1,M1,KH)
12 AA(LT,M1)=X*U
        DO 14 MM=1,LMP1
          X=0.
          DO 15 IH=1,LIFI
            KH=NRH(IH)
15 X=X+XK(LMN1,LT,KH)*FEX(LM,MM,IH)
14 B(LT,MM)=X
11 CONTINUE
    IF(LTL.GT.1) GOTO 16
    AQ(1,1)=1.0/AA(1,1)
    GOTO 17
16 CONTINUE
    IF(LTL.GT.2) GO TO 83
    DETIN=1.0/(AA(1,1)*AA(2,2)-AA(1,2)*AA(2,1))
    AQ(1,1)=DETIN*AA(2,2)
    AQ(1,2)=-DETIN*AA(2,1)
    AQ(2,1)=-DETIN*AA(1,2)
    AQ(2,2)=DETIN*AA(1,1)
    GO TO 17
83 CONTINUE
  Q1=AA(1,1)
  Q2=AA(1,2)
  Q3=AA(1,3)
  Q4=AA(2,1)
  Q5=AA(2,2)
  Q6=AA(2,3)
  Q7=AA(3,1)
  Q8=AA(3,2)
  Q9=AA(3,3)
  DETIN=1.0/(Q1*Q5+Q9+Q4*Q8+Q3+Q2*Q7+Q6+QX+Q5+Q7+Q8+Q6+Q1+Q4+Q2+Q9)

```

```

DO 32 MM=1,LMP1
  WRITE(LOUT,1002) MM,(C(LMN1,M1,MM),DC(MM,M1),M1=1,LTL)
32 CONTINUE
  WRITE(LOUT,1007) (NOR(I),I=1,LMP1)
  WRITE(LOUT,1004) (DFA(MM),MM=1,LMP1)
  WRITE(LOUT,1008) CM,DCM,DMMF,CN
  Z=Z+CN
10 CONTINUE
  WRITE(LOUT,1009) Z
  WRITE(LTP,2010) ACT
  WRITE(LTP,2015) (HEAD(I),I=1,LOK)
  DO 33 LM=2,L
    LMP1=LM+1
    LMN1=LM-1
    LTL=M(LM)
    DO 33 MM=1,LMP1
33 WRITE(LTP,1003) (C(LMN1,M1,MM),M1=1,LTL)
    IF(LMB.NF.1) GO TO 100
    WRITE(LMB) ACT,HEAD
    WRITE(LMB) C
100 CONTINUE
    RETURN
1000 FORMAT(1H ///20H C AND DC MATRICES)
1001 FORMAT(1H1///1H ,7H L = ,I6)
1002 FORMAT(1H ///1H ,I10,5X,4(F15.6,F15.6,5X))
1003 FORMAT(8F10.4)
1004 FORMAT(1H /3(1H ,8F13.5/))
1005 FORMAT(1H ///1H ,4(33X,I2))
1006 FORMAT(1H ///1H ,8X,2HN1,5X,4(8X,1HC,13X,2HDC,11X))
1007 FORMAT(1H ///1H ,12H DF VECTOR///3(1H ,8I13/))
1008 FORMAT(1H ///1H ,9X,6HC=MEAN,14X,7HDC=MEAN,12X,7HDF=MEAN,12X,2HCN/
  +/4F20.5)
1009 FORMAT(1H1/////1H ,5X,22HTEXTURE INDEX J = ,F13.5)
2010 FORMAT(10A8)
2015 FORMAT(F10.0,7(A8,2X)/2F10.0/4(3F10.0/))
7000 FORMAT(1H1///1H ,54X,12HCOEFFICIENTS/1H ,52X,16(1H*)/////1H ,5X,0
  *NOTATIONS///1H ,5X,51HC THREE DIMENSIONAL FUNCTION COE
  *FFICIENTS///1H ,5X,23HDC DISPERSIONS C ///1H ,5X,53HDF
  *F EXPERIMENTAL COEFFICIENTS DISPERSIONS///1H ,5X,89HC=MEAN
  * MEAN VALUE OF C COEFFICIENTS FOR DEFINITE VALUE
  * OF L INDEX///1H ,5X,90HDC=MEAN MEAN VALUE OF DC D
  *ISPERSIONS FOR DEFINITE VALUE OF L INDEX///1H ,5X,90HD
  *F=MEAN MEAN VALUE OF DF DISPERSIONS FOR DEFINITE
  * VALUE OF L INDEX///1H ,5X,114HCN SUM OF SQUARE VA
  *LUFS OF C COEFFICIENTS FOR DEFINITE VALUE OF L D
  *EVIDED BY 2*L+1////////)
  END
7.4. POLO
SUBROUTINE POLO
  REAL NO
  DIMENSION CCS(307),A(40),D(18,18),F(18),NO(18),M(17),NOR(18),XP(20
  *,20)
  COMMON FEX(17,18,4),R(19,19)
  COMMON /SET/ IN,INP,LIB,LOUT,LTP,LMB
  COMMON /DAT/ HEAD(22),ACT(10)
  COMMON /PAR/ LMAX,LFMAX
  COMMON /ORG/ LIFI,LOK,J,I
  DATA PI/12.56637/
  DATA M/0.1,1,1,1,2,1,2,2,2,2,3,2,3,3,3,3/

```



```

AQ(1,1)=DETIN*(Q5+Q9-Q6+Q8)
AQ(1,2)=DETIN*(Q6+Q7-Q4+Q9)
AQ(1,3)=DETIN*(Q4+Q8-Q5+Q7)
AQ(2,1)=DETIN*(Q3+Q8-Q2+Q9)
AQ(2,2)=DETIN*(Q1+Q9-Q3+Q7)
AQ(2,3)=DETIN*(Q2+Q7-Q1+Q8)
AQ(3,1)=DETIN*(Q2+Q6-Q3+Q5)
AQ(3,2)=DETIN*(Q3+Q4-Q1+Q6)
AQ(3,3)=DETIN*(Q1+Q5-Q2+Q4)
17 CONTINUE
DO 18 MM=1,LMP1
DO 19 M1=1,LTL
X=0.
DO 20 LT=1,LTL
20 X=X+AQ(M1,LT)*B(LT,MM)
C(LMN1,M1,HT)=X
19 CONTINUE
18 CONTINUE
DO 21 IH=1,LIFI
KH=NRH(IH)
DO 22 MM=1,LMP1
X=0.
DO 23 M1=1,LTL
23 X=X+C(LMN1,M1,HT)*XK(LIN1,M1,KH)
22 F1(MM,IH)=H*X
21 CONTINUE
DO 26 MM=1,LMP1
X=0.
DO 27 KH=1,LIFI
Y=FEX(LM,MM,KH)-F1(MM,KH)
27 X=X+Y*Y
Y=X/FLOAT(LIFI-LTL)
DFA(MM)=SORT(X)
DO 28 M1=1,LTL
28 DC(MM,M1)=DFA(MM)*SORT(AQ(M1,M1)/Y)
26 CONTINUE
DMFM=0.
DCM=0.
CM=0.
CH=0.
DO 29 MM=1,LMP1
DMFM=DMFM+ABS(DFA(MM))
DO 30 M1=1,LTL
DCM=DCM+ABS(DC(MM,M1))
XR=C(LMN1,M1,MM)
CM=CM+ABS(XR)
CH=CH+XR**2
30 CONTINUE
29 CONTINUE
DMFM=DMFM/FLOAT(LM+1)
DCM=DCM/FLOAT((LM+1)*LTL)
CM=CM/FLOAT((LM+1)*LTL)
CH=CH/(4.0*LM+1.0)
DO 31 KH=1,LIFI
DO 31 FM=1,LMP1
31 FEX(LM,HT,KH)=F1(FM,KH)
L22=2*LM
WRITE(LOUT,1001) LM22
WRITE(LOUT,1000)
WRITE(LOUT,1005)(I,I=1,LTL)

```

```

DATA NO/.398942,17*.564190/
DATA NOR/1,2,3,4,5,6,7,8,9,10,11,12,13,14,15,16,17,18/
DATA YB/0.17453293/
IF(LIFI,NE,1) GO TO 50
DO 14 I=1,307
14 CCS(I)=COS(YB*FLOAT(I-1))
JDR=19
IDR=19
XP(1,1)=0.
DO 8 I=2,20
XX=5.*FLOAT(I-2)
XP(I,1)=XX
8 XP(1,I)=XX
50 CONTINUE
DO 21 I=1,100
21 READ(LIB)
LPM1=LMAX+1
DO 19 N=1,LPM1
DO 19 IS=1,LPM1
19 D(N,IS)=0.
DO 20 L=2,LMAX
LP1=L+1
DO 25 N=1,LP1
READ(LIB) A
X=NO(N)*FEX(L,N,LIFI)
DO 25 IS=1,LP1
25 D(N,IS)=D(N,IS)+X*A(IS)
20 CONTINUE
REWIND LIB
DO 30 ID=1,IDR
ID1=ID-1
DO 35 N=1,LPM1
X=0.
DO 40 IS=1,LPM1
ID2=(IS-1)*ID1+1
40 X=X+D(N,IS)*CCS(ID2)
35 E(N)=X
DO 30 JD=1,JDR
Y=0.
JD1=JD-1
DO 45 N=1,LPM1
JD2=(N-1)*JD1+1
45 Y=Y+E(N)*CCS(JD2)
30 XP(JD+1,ID+1)=1.+Y
LIP=11+3*(LIFI-1)
WRITE(IOUT,1006) HEAD(LIP)
WRITE(IOUT,1030) (NOR(N),N=1,LPM1)
DO 47 L=2,LMAX
LP1=L+1
L2=2*L
47 WRITE(LOUT,1020) L2,(FEX(L,N,LIFI),N=1,LP1)
WRITE(IOUT,1005) HEAD(LIP)
WRITE(IOUT,1010)((XP(J,I),J=1,20),I=1,20)
RETURN
1005 FORMAT(1H1///35H CALCULATED POLE FIGURE HKL=F5.0//)
1006 FORMAT(1H1///49H TABLE F FOR CALCULATED POLE FIGURE
      *F6.0//)
1010 FORMAT(1H ,20F6.1//)
1020 FORMAT(1H /1H ,I10,10F10.4/1H ,10X,10F10.4)
1030 FORMAT(1H /1H ,10X,10I10/1H ,10X,10I10)
END

```

7.5. POLV

```

SUBROUTINE POLV(IQUAN,JQUAN)
  INTEGER HKL
  REAL NO
  DIMENSION CCS(307)
  DIMENSION AAA(16,18,18),XK(16,5,8),XP(20,20),F1(16,18),D(18,18),
  *E(18),MODHKL(8),      NO(18),M(17),A(40),NOR(18)
  COMMON CCS,AAA,XK,XP
  COMMON /SET/ IN,INP,LIB,IOUT,LTP,LMB
  COMMON /DAT/ HEAD(22),ACT(10)
  COMMON /PAR/ LMAX,LFMAX
  COMMON /EVD/ C(16,3,18)
  DATA YB/U.17453293/
  DATA NOR/1,2,3,4,5,6,7,8,9,10,11,12,13,14,15,16,17,18/
  DATA NO/.398942,17*.564190/
  DATA M/0,1,1,1,1,1,2,1,2,2,2,2,3,2,3,3,3,3/
  DATA PI/12.56637/
  DATA MODHKL/100,110,111,102,112,122,103,113/
  READ(IN,1001) XHKL,XLMAX
  HKL=FIX(XHKL)
  LMAX=INT((XLMAX+.0001)/2.)
  IF(JQUAN.NE,1) GO TO 55
  CALL XDATA
55 CONTINUE
  IF(IQUAN.NE,1) GO TO 50
  DO 14 I=1,307
14  CCS(I)=COS(YB*FLOAT(I-1))
  JDR=19
  IDR=19
  XP(1,1)=0.
  DO 8 I=2,20
  XX=5.*FLOAT(I-2)
  XP(1,1)=XX
  8  XP(1,I)=XX
  DO 21 I=1,1/0
21  READ(LIB)
  READ(LIB) XK
  DO 22 I=1,19
22  READ(LIB)
  DO 2 L=1,16
  LP2=L+2
  DO 2 N=1,LP2
  READ(LIB) A
  DO 2 IS=1,LP2
  2  AAA(L,N,IS)=A(IS)
  REWIND LIB
50 CONTINUE
  DO 5 K2=1,8
  IF(MODHKL(K2).EQ,HKL) GO TO 6
  5  CONTINUE
  6  KH=K2
  DO 11 L=2,LMAX
  LP1=L+1
  LN1=L-1
  LTL=M(L)
  U=PI/(FLOAT(L)*4.+1.0)
  DO 11 N=1,LP1

```

7.6. UNKC

```

SUBROUTINE UNKC(IQUAN)
  DIMENSION BU(16,3,9),D(9,18,35)
  DIMENSION E(18,35),G(18),H(18),SLN(631)
  DIMENSION XP(20,20),MO(17),A(40)
  COMMON SLN
  COMMON /SET/ IN,INP,LIB,IOUT,LTP,LMB
  COMMON /DAT/ HEAD(22),ACT(10)
  COMMON /PAR/ LMAX,LFMAX
  COMMON /EVD/ C(16,3,18)
  DATA MO/U.1,1,1,1,1,2,1,2,2,2,2,3,2,3,3,3,3/
  DATA XPF1/8HF1PR /
  DATA B/U.087266465/
  EQUIVALENCE (LO,IOUT)
  READ(IN,1000) XPRO,XLMAX,XLF1,XLF2
  LMAX=INT((XLMAX+.0001)/2.)
  LF1=INT((XLF1+.0001)/5.)*1
  LF2=INT((XLF2+.0001)/5.)*1
  CALL XDATA
  IF(IQUAN.NE,1) GO TO 50
  DO 3 J=1,631
  3  SLN(J)=SIN(FLOAT(J-1)*B)
50 CONTINUE
  LMT0=LMAX/2+1
  LMT1=LMAX+1
  LMT2=LMAX*2+1
  DO 1 MM=1,LMT0
  DO 1 N=1,LMT1
  DO 1 IS=1,LMT2
  1  D(MM,N,IS)=0.0
  DO 4 J=1,358
  4  READ(LIB)
  READ(LIB) BU
  DO 20 IF1=2,20
  XX=FLOAT(IF1-2)*5.
  XP(IF1,1)=XX
  20  XP(1,IF1)=XX
  DO 8 L=2,LMAX
  MUP=L/2+1
  LP1=L+1
  LN1=L-1
  LT2=L*2+1
  LTL=MO(L)
  DO 8 MM=1,MUP
  DO 8 N=1,LP1
  X=0.
  DO 9 M1=1,.TL
  9  X=X+C(LN1,M1,N)*BU(LN1,M1,MM)
  IF(N.NE,1) X=X*1.4142135
  READ(LIB) A
  DO 10 IS=1,LT2
  10  D(MM,N,IS)=D(MM,N,IS)+X*A(IS)
  8  CONTINUE
  REWIND LIB
  IF(XPRO.EQ,XPF1) GO TO 200
  WRITE(LU,1002)
  LD2=LMAX/2+1
  LMA1=LMAX+1

```

```

X=0.0
DO 12 M1=1, LTL
12 X=X+C(LN1,M1,N)*XK(LN1,M1,KH)
F1(LN1,N)=X+U
11 CONTINUE
LP1=LMAX+1
WRITE(IOUT,1006) MODHKL(KH)
WRITE(IOUT,1030)(NOR(I),I=1,LP1)
DO 47 L=2, LMAX
LP1=L+1
LP2=L-1
L2=2*L
47 WRITE(IOUT,1020) L2,(F1(LP2,N),N=1,LP1)
LPM1=LMAX+1
DO 19 N=1, LPM1
DO 19 IS=1, LPM1
19 D(N,IS)=.0
DO 20 L=2, LMAX
LP1=L+1
LN1=L-1
DO 25 N=1, LP1
X=NO(N)*F1(LN1,N)
DO 25 IS=1, LP1
25 D(N,IS)=D(N,IS)+X*AAA(LN1,N,IS)
20 CONTINUE
DO 30 ID=1, IDR
ID1=ID-1
DO 35 N=1, LPM1
X=.0
DO 40 IS=1, LPM1
ID2=(IS-1)*ID1+1
40 X=X+D(N,IS)*CCS(ID2)
35 E(N)=X
DO 30 JD=1, JDR
Y=.0
JD1=JD-1
DO 45 N=1, LPM1
JD2=(N-1)*JD1+1
45 Y=Y+E(N)*CCS(JD2)
30 XP(JD+1,ID+1)=1.+Y
WRITE(IOUT,1005) MODHKL(KH)
WRITE(IOUT,1010)((XP(J,I),J=1,20),I=1,20)
RETURN
1001 FORMAT(2F10.0)
1005 FORMAT(1H1///30H CALCULATED POLE FIGURE ,110//)
1006 FORMAT(1H1///49H TABLE F FOR CALCULATED POLE FIGURE
* 110//)
1010 FORMAT(1H ,20F6.1//)
1020 FORMAT(1H /1H ,110,10F10.4/1H ,10X,10F10.4)
1030 FORMAT(1H /1H ,10X,10I10/1H ,10X,10I10)
END

```

```

IPS=4
JPS=2
GO TO 300
200 CONTINUE
WRITE(L0,1005)
LD2=LMAX+1
LMA1=LMAX/2+1
IPS=2
JPS=4
300 CONTINUE
DO 100 IF2=LF1,LF2
XP(1,1)=5.*FLOAT(IF2-1)
DO 11 N=1, LMA1
IV=1
DO 12 IS=1, LMT2
X=.0
I=9+9*IV
DO 13 M=1, LD2
IF(XPRO,EQ,XPF1) GO TO 400
K=M
J=N
GO TO 500
400 CONTINUE
K=N
J=M
500 CONTINUE
LH=IPS*(M-1)*(IF2-1)+1+I
13 X=X+D(K,J,IS)*SLN(LH)
E(N,IS)=X
IV=-IV
12 CONTINUE
11 CONTINUE
DO 14 IF=1,19
DO 15 N=1, LMA1
X=.0
Y=E(N,1)
DO 16 IS=2, LMT2,2
LH=(IS-1)*(IF-1)+19
LH1=IS*(IF-1)+19
X=X+E(N,IS)*SLN(LH)
16 Y=Y+E(N,IS+1)*SLN(LH1)
G(N)=Y
15 H(N)=X
DO 17 IF1=1,19
Z=.0
DO 18 N=1, LMA1
LH=JPS*(N-1)*(IF1-1)+1
18 Z=Z+G(N)*SLN(LH+18)-H(N)*SLN(LH)
XP(IF+1,IF1+1)=1.0+2.50662827*Z
17 CONTINUE
14 CONTINUE
WRITE(IOUT,1005)((XP(IF,IF1),IF1=1,20),IF=1,20)
100 CONTINUE
RETURN
1000 FORMAT(A8,2X,3F10.0)
1002 FORMAT(1H1///65H DISTRIBUTION FUNCTION OF THREE PARAMETERS
* PROJECTION F2///)
1003 FORMAT(1H1///65H DISTRIBUTION FUNCTION OF THREE PARAMETERS
* PROJECTION F1///)
1005 FORMAT(1H1///^(20F6.1//))
END

```

7.7. INVA

```

SUBROUTINE INVA(IQUAN)
  REAL NO
  DIMENSION M(17),NO(18),E(9),XT(7),U(8),A(40),XKK(18),T(409)
  DIMENSION D(9,18),H(16,3),B(16,3,9),AA(16,18,18),XP(20,26)
  COMMON T,AA,B,XP
  COMMON /SET/ IN,INP,LIB,IOUT,LTP,LMB
  COMMON /DAT/ HEAD(22),ACT(10)
  COMMON /PAR/ LMAX,LFMAX
  COMMON /EVD/ C(16,3,18)
  DATA NO/U,398942,17*0.564190/
  DATA PI/12,56637/
  DATA PIII/3,14159265/
  DATA YB/U,017453293/
  DATA U(1),U(2),U(4)/3*.0/
  DATA U(3),U(5),U(6)/3*1.57079633/
  DATA XT(1)/8H NORMAL /
  DATA XT(3)/8H ROLLING/
  DATA XT(5)/8H TRANSVER/
  DATA XT(7)/8H CHOOSEN/
  DATA M/U,1,1,1,1,1,2,1,2,2,2,3,2,3,3,3,3/
  DATA XSTND/8HSTND /
  DATA XROLL/8HROLL /
  DATA XNORM/8HNORM /
  DATA XTRAN/8HTRAN /
  DATA XDIRC/8HDIRC /
  EQUIVALENCE(IOUT,LOUT)
  READ(IN,1000) XWAY,XLMAX
  LMAX=INT((XLMAX+.0001)/2.)
  IF(XWAY,EQ,XSTND) GO TO 600
  IF(XWAY,EQ,XROLL) GO TO 601
  IF(XWAY,EQ,XNORM) GO TO 602
  IF(XWAY,EQ,XTRAN) GO TO 603
  IF(XWAY,EQ,XDIRC) GO TO 604
600 CONTINUE
  IPINV2=5
  IPINV1=1
  GO TO 666
601 CONTINUE
  IPINV1=3
  IPINV2=3
  GO TO 666
602 CONTINUE
  IPINV1=1
  IPINV2=1
  GO TO 666
603 CONTINUE
  IPINV1=5
  IPINV2=5
  GO TO 666
604 CONTINUE
  IPINV1=7
  IPINV2=7
  READ(IN,1001) U(7),U(8)
  U(7)=YB*U(7)
  U(8)=YB*U(8)
666 CONTINUE
  CALL XDATA
  IF(IQUAN.NE,1) GO TO 50
  I=25

```

```

  DO 30 L=2,LMAX
  LP1=L+1
  LM=L/2+1
  LTL=M(L)
  LN1=L-1
  DO 30 MM=1,LM
  MM2=2*(MM-1)+1
  X=.0
  DO 31 M1=1,LTL
  51 X=X+H(LN1,M1)*B(LN1,M1,MM)
  DO 32 IS=1,LP1
  52 D(MM,IS)=D(MM,IS)+X*AA(LN1,MM2,IS)
  50 CONTINUE
  LMP1=LMAX+1
  LMM1=LMAX/2+1
  DO 40 I=1,I1
  IP=I-1
  DO 41 MM=1,LMM1
  X=.0
  DO 42 IS=1,LMP1
  ISP=(IS-1)*IP+1
  42 X=X+D(MM,IS)*T(ISP)
  41 E(MM)=X
  DO 45 J=1,J1
  X=.0
  JP=J-1
  DO 46 MM=1,LMM1
  MJ=2*(MM-1)+JP+1
  46 X=X+E(MM)*T(MJ)
  XP(J+1,I+1)=1,+X
  45 CONTINUE
  40 CONTINUE
  WRITE(LOUT,1002) XT(IPINV)
  WRITE(LOUT,1005) ((XP(J,I),J=1,J11),I=1,I11)
  10 CONTINUE
  RETURN
1000 FORMAT(A8,2X,F10.0)
1001 FORMAT(8F10,5)
1002 FORMAT(1H1///32H INVERSE POLE FIGURE OF THE ,A8,11H DIRECTION
  *//)
1003 FORMAT(1H /1H ,8H THETA =,F10.2//9H PSI =,F10.2//)
1004 FORMAT(1H /1H ,110,3F10,4)
1005 FORMAT(1H ,20F6,1//)
1006 FORMAT(1H1///49H TABLE H FOR INVERSE FIGURE OF THE
  * A8,11H DIRECTION //)
1007 FORMAT(1H /1H ,10X,3I10)
  END

```

7.8. SETS

```

SUBROUTINE SETS
  REAL INDEV
  COMMON /SET/ IN,INP,LIB,IOUT,LTP,LMB
  DATA XSET/8HTAPE /
  DATA YSET/8HCARD /
  DATA ZSET/8HMAGB /
  IOUT=3
  LIB=7
  LTP=5
  LMB=5
  READ(IN,6666) INDEV,OUTDEV

```

```

I11=26
J1=19
J11=20
YB1=5,*YB
DO 99 I=1,409
99 T(I)=COS(YB1*FLOAT(I-1))
DO 2 I=1,190
2 READ (LIB)
DO 6 L=2,17
LP1=L+1
LN1=L-1
DO 6 N=1,LP1
READ(LIB)A
DO 7 IS=1,LP1
7 AA(LN1,N,IS)=A(IS)
6 CONTINUE
READ(LIB)B
REWIND LIB
XP(1,1)=0,
DF=2,5
DO 100 I=2,26
100 XP(1,I)=DF*FLOAT(I-2)
DO 200 J=2,20
200 XP(J,1)=DF*FLOAT(J-2)
50 CONTINUE
DO 10 IPINV=IPINV1,IPINV2,2
IPI=IPINV-IPINV/2
U1=2,*U(IPINV)
U2=2,*U(IPINV+1)
DO 11 L=2,LMAX
UX=PI/(FLOAT(L)*4.+1.)
LP1=L+1
LN1=L-1
DO 12 N=1,LP1
X=0,
DO 13 IS=1,LP1
13 X=X+AA(LN1,N,IS)*COS(U1*FLOAT(IS-1))
12 XXX(N)=X*NU(N)*COS(U2*FLOAT(N-1))
LTL=M(L)
DO 14 M1=1,LTL
X=0,
DO 15 N=1,LP1
15 X=X+XXX(N)*C(LN1,M1,N)
14 H(LN1,M1)=UX*X
11 CONTINUE
WRITE(LOUT,1006) XT(IPINV)
IF(IPINV.NE.7) GO TO 55
U(7)=U(7)/YB
U(8)=U(8)/YB
WRITE(LOUT,1003) U(7),U(8)
55 CONTINUE
IR=M(LMAX)
WRITE(LOUT,1007) (I,I=1,IR)
DO 60 L=2,LMAX
LN1=L-1
LTL=M(L)
LL=2+L
60 WRITE(LOUT,1004) LL,(H(LN1,M1),M1=1,LTL)
DO 20 MM=1,9
DO 20 IS=1,18
20 D(MM,IS)=0

```

```

IF(INDEV.EQ,XSET) INP=4
IF(INDEV.EQ,YSET) INP=2
IF(INDEV.EQ,ZSET) INP=6
IF(OUTDEV.EQ,ZSET) LMB=1
RETURN
6666 FORMAT(A8,2X,A8)
END

```

7.9. CAPITE

```

SUBROUTINE CAPITE(NAME)
COMMON /SET/ IN,INP,LIB,IOUT,LTP,LMB
COMMON /DAT/ HEAD(22),ACT(10)
COMMON /PAR/ LMAX,LFMAX
CALL DATE(XDATE)
IF(INP.NE.6) GO TO 666
READ(INP) ACT,HEAD
LFMAX=IFIX(HEAD(9))
LMAX=INT((HEAD(10)+.0001)/2)
J1=10+3*LFMAX
GO TO 606
666 CONTINUE
READ(INP,6666) ACT
READ(INP,6000) (HEAD(J),J=1,10)
LFMAX=IFIX(HEAD(9))
LMAX=INT((HEAD(10)+.0001)/2)
J1=10+3*LFMAX
READ(INP,6006) (HEAD(J),J=11,J1)
READ(INP,6007)
606 CONTINUE
WRITE(IOUT,6001)
WRITE(IOUT,6002) NAME
WRITE(IOUT,6003) HEAD(1)
WRITE(IOUT,6004) (ACT(J),J=1,10),XDATE
WRITE(IOUT,6005) (HEAD(J),J=3,J1)
WRITE(IOUT,6066) HEAD(2)
RETURN
6000 FORMAT(F10.0,7(A8,2X)/2F10.0)
6001 FORMAT(1H1////1H,37X,46HTHREE DIMENSIONAL ANALYSIS OF T
*EXTURES/1H,36X,48(1H*)////1H)
6002 FORMAT(1H,39X,A4,38H PROGRAM --- VERSION FEBRUARY 1973/1H,36
*X,48(1H*)////1H)
6003 FORMAT(1H,48X,18HDATA BLOCK NO.,F6.0/1H,48X,24(1H*)////1H)
6004 FORMAT(1H,8X,104(1H*)/1H,8X,1H*,102X,1H*/1H,8X,1H*,3X,10A8,8X,A
*9,2X,1H*/1H,8X,1H*,102X,1H*/1H,8X,104(1H*)/1H)
6005 FORMAT(1H,20X,12HMEASURED ,A8,10X,12HMEASURED ,A8,10X,12HLA
*BURATORY ,A8/1H,20X,8(1H*),22X,8(1H*),22X,10(1H*)/1H,35X,20HSP
*ECIMEN DATA ,3(A8,2X)/1H,35X,14(1H*)/1H,25X,39H NUMBER
*OF MEASURED POLE FIGURES ,F4.0,4X,19HMAXIMAL L VALUE ,F4.0/
*1H,27X,35(1H*),10X,17(1H*)/1H,30X,23Hkind OF POLE FIGURES,1
*7X,15HANGULAR STEPS/1H,30X,23(1H*),10X,29(1H*)/1H,39X,5H HKL
*,21X,5HD-ALF,15X,5HD-BET//4(1H,24X,F20.0,6X,2F20.0//),1H)
6006 FORMAT(3F10.0)
6007 FORMAT(1X)
6066 FORMAT(1H//1H,10X,10HPROGRAMMER,4X,A8/1H,8X,104(1H*)/1H,8X,104
*(1H*)////1H)
6666 FORMAT(10A8)
END

```

7.10. XDATA

```

SUBROUTINE XDATA
  DIMENSION MU(17),NO(18)
  COMMON /SET/ IN,INP,LIB,IOUT,LTP,LMB
  COMMON /DAT/ HEAD(22),ACT(10)
  COMMON /PAR/ LMAX,LFMAX
  COMMON /EVD/ C(16,3,18)
  DATA MO/0,1,1,1,1,2,1,2,2,2,2,3,2,3,3,3,3/
  DATA NO/1,2,3,4,5,6,7,8,9,10,11,12,13,14,15,16,17,18/
  LX=LMAX+1
  WRITE(IOUT,1010)(NO(IK),IK=1,LX)
  LMAX2=IFIX(HEAD(10))/2
  IF(INP.NE.6) GO TO 666
  READ(INP) C
666 CONTINUE
  DO 1 L=2,LMAX2
    IF(L.GT.LMAX) GO TO 444
    LN1=L-1
    LP1=L+1
    LTL=MU(L)
    L2=2*L
    IF(INP.EQ.6) GO TO 555
    DO 4 N=1,LP1
      READ(INP,1001)(C(LN1,M1,N),M1=1,LTL)
555 CONTINUE
    DO 5 M1=1,LTL
      WRITE(IOUT,1100) L2,M1,(C(LN1,M1,N),N=1,LP1)
    1 CONTINUE
444 CONTINUE
    RETURN
1001 FORMAT(8F10,4)
1010 FORMAT(1H1//31H MATRIX C COEFFICIENTS //1H ,10X,12(16,3X)
  *//1H ,10X,12(16,3X)/)
1100 FORMAT(1H //1H ,2X,214,12F9.4/1H ,10X,12F9.4/)
END

```

7.11. PING

```

MASTER PING
COMMON WORK(1585)
COMMON /SET/ IN,INP,LIB,IOUT,LTP,LMB
COMMON /DAT/ HEAD(22),ACT(10)
COMMON /PAR/ LMAX,LFMAX
COMMON /OEG/ LIFI,LOK,J,I
DATA NAME/4PPING/
DATA XINIT/8HINIT //, XEXOD/8HEXOD
IN=2
777 READ(IN,1111) REQST
IF(REQST.EQ.XINIT) GO TO 770
IF(REQST.EQ.XEXOD) GO TO 707
GO TO 777
770 CONTINUE
LOK=10
CALL SETS
CALL CAPITE(NAME)
DO 1 LIFI=1,LFMAX
  CALL CORFL
  CALL TWODIM
1 CONTINUE
CALL COEF
DO 2 LIFI=1,LFMAX

```

7.13. INVE

```

MASTER INVE
COMMON WORK(6545)
COMMON /SET/ IN,INP,LIB,IOUT,LTP,LMB
COMMON /DAT/ HEAD(22),ACT(10)
COMMON /PAR/ LMAX,LFMAX
COMMON /EVD/ C(16,3,18)
DATA NAME/4HINVE/
DATA XINIT/8HINIT //, XEXOD/8HEXOD
DATA IQUAN/1/
IN=2
777 READ(IN,1111) REQST
IF(REQST.EQ.XINIT) GO TO 770
IF(REQST.EQ.XEXOD) GO TO 707
GO TO 777
770 CONTINUE
CALL SETS
CALL CAPITE(NAME)
CALL INVA(IQUAN)
IQUAN=2
GO TO 777
707 WRITE(IOUT,2000)
STOP
1111 FORMAT(A8)
2000 FORMAT(1H1//////////1H ,50X,21HTEXTUR NORMAL END/1H1)
END

```

7.14. FUNE

```

MASTER FUNE
COMMON WORK(631)
COMMON /SET/ IN,INP,LIB,IOUT,LTP,LMB
COMMON /DAT/ HEAD(22),ACT(10)
COMMON /PAR/ LMAX,LFMAX
COMMON /EVD/ C(16,3,18)
DATA XINIT/8HINIT //, XEXOD/8HEXOD
DATA NAME/4HFUNE/
DATA IQUAN/1/
IN=2
777 READ(IN,1111) REQST
IF(REQST.EQ.XINIT) GO TO 770
IF(REQST.EQ.XEXOD) GO TO 707
GO TO 777
770 CONTINUE
CALL SETS
CALL CAPITE(NAME)
CALL UNKC(IQUAN)
IQUAN=2
GO TO 777
707 WRITE(IOUT,2000)
STOP
1111 FORMAT(A8)
2000 FORMAT(1H1//////////1H ,50X,21HTEXTUR NORMAL END/1H1)
END

```

```

      CALL POLD
2  CONTINUE
      GO TO 777
707  WRITE(IOUT,2000)
      IF(LMB.NE.1) GO TO 3
      ENDFILE LMB
      REWIND LMB
3  CONTINUE
      STOP
1111  FORMAT(A8)
2000  FORMAT(1H1//////////1H ,50X,21HTEXTUR  NORMAL  END/1H1)
      END

```

7.12. POLF

```

MASTER POLF
COMMON WORK(6275)
COMMON /SET/ IN,INP,LIB,IOUT,LTP,LMB
COMMON /DAT/ HEAD(22),ACT(10)
COMMON /PAR/ LMAX,LFMAX
COMMON /EVD/ C(16,3,18)
DATA XINIT/8HINIT /, XEXOD/8HEXOD
DATA XNEXT/8HNEXT /
DATA NAME/4HPOLF/
DATA IQUAN/1/
IN=2
777  READ(IN,1111) REQST
      IF(REQST.EQ,XINIT) GO TO 770
      IF(REQST.EQ,XNEXT) GO TO 700
      IF(REQST.EQ,XEXOD) GO TO 707
      GO TO 777
770  CONTINUE
      JQUAN=1
      CALL SETS
      CALL CAPITE(NAME)
700  CONTINUE
      CALL POLV(IQUAN,JQUAN)
      IQUAN=2
      JQUAN=2
      GO TO 777
707  WRITE(IOUT,2000)
      STOP
1111  FORMAT(A8)
2000  FORMAT(1H1//////////1H ,50X,21HTEXTUR  NORMAL  END/1H1)
      END

```

7.15. LIBR

```

MASTER LIBR
DIMENSION AK(17,18,18),ANS(35,18),BB(16,5,9),XK(16,5,8)
DIMENSION A(40),BAW(40),XBB(432),ZK(384)
DIMENSION MO(17),MODHKL(8)
DIMENSION HELP(20)
DATA XBB/432*0.0/,ZK/384*0.0/
DATA MO/0,1,1,1,1,2,1,2,2,2,3,2,3,3,3,3/
DATA MODHKL/100,110,111,102,112,122,103,113/
EQUIVALENCE (XBB(1),BB(1,1,1)),(ZK(1),XK(1,1,1))
INP=2
IOUT=3
LIB=7
DO 2 J=1,40
  A(J)=0
2 BAW(J)=0
  WRITE(IOUT,1100)
  WRITE(IOUT,2000)
  DO 11 L=1,17
    WRITE(IOUT,2200)
    LP1=L+1
    DO 11 N=1,LP1
      WRITE(IOUT,2200)
      READ(INP,1000) (HELP(LIS),LIS=1,LP1)
      DO 111 LIS=1,LP1
111 AK(L,N,LIS)=HELP(LIS)
      DO 12 I=1,19
        X=HELP(I)
        XI=0.17453293*FLOAT(I-1)
        DO 20 IS=2,LP1
20 X=X+HELP(IS)*COS((IS-1)*XI)
        BAW(I)=X
12 CONTINUE
        WRITE(IOUT,1001) (BAW(I),I=1,19)
        WRITE(LIB) BAW
11 CONTINUE
        WRITE(IOUT,3000)
        DO 201 J=1,8
          WRITE(IOUT,2500) MODHKL(J)
          DO 202 K=1,16
            LTL=MO(K+1)
202 READ(INP,1000) (XK(K,I,J),I=1,LTL)
            DO 203 K=1,16
              WRITE(IOUT,2200)
              LTL=MO(K+1)
203 WRITE(IOUT,1001) (XK(K,I,J),I=1,LTL)
201 CONTINUE
          WRITE(LIB) XK
          DO 4 J=1,17
4 WRITE(LIB) A
          WRITE(IOUT,4000)
          DO 301 L=1,17
            WRITE(IOUT,2200)
            LP1=L+1
            DO 301 N=1,LP1
              WRITE(IOUT,2200)
            DO 310 IS=1,LP1
310 A(IS)=AK(L,N,IS)
            WRITE(IOUT,1001) (A(IS),IS=1,LP1)
            WRITE(LIB) A
301 CONTINUE
          WRITE(IOUT,5000)
          DO 401 L=2,17
            WRITE(IOUT,2200)
            LN1=L-1
            LPOL=L/2+1
            LTL=MO(L)

```

```

DO 401 ML=1,LTL
  READ(INP,1000) (BB(LN1,ML,N),N=1,LPOL)
  WRITE(IOUT,2200)
401 WRITE(IOUT,1001) (BB(LN1,ML,N),N=1,LPOL)
  WRITE(LIB) BB
  DO 10 J=1,40
10 A(J)=0,0
    WRITE(IOUT,6000)
    DO 900 L=2,17
      WRITE(IOUT,2200)
      LP1=L+1
      LP2=2*L+1
      LP3=L/2+1
      XJJ=FLOAT(2*L)
      DO 200 N=1,LP2,2
        INK=N/2+1
        DO 200 IS=1,LP1
          ANS(N,IS)=AK(L,INK,IS)
200 CONTINUE
        DO 300 N=2,LP2,2
          ANS(N,1)=0,0
          XNN=FLOAT(N-1)
          XN2=XJJ-XNN
          XN3=XJJ+XNN
          Z1=SQRT(XN2*(XN3+1,0))
          Z2=SQRT(XN3*(XN2+1,0))
          DO 300 IS=2,LP1
            ANS(N,IS)=(Z1*ANS(N+1,IS)+Z2*ANS(N-1,IS))/(4.0*FLOAT(IS-1))
300 CONTINUE
        DO 400 N=1,LP2,2
          ANS(N,1)=2.0*ANS(N,1)
400 CONTINUE
        X=SQRT(2.0/(2.0*XJJ+1,0))*ANS(1,1)
        DO 500 M=1,LP3
          WRITE(IOUT,2200)
          V1=1,0
          MM=2*M-1
          A1=X/ANS(4*M-3,1)
          DO 600 N=1,LP1
            WRITE(IOUT,2200)
            A2=A1*V1/ANS(2*N-1,1)
            DO 700 IS=1,LP2
              X1=ANS(IS,MM)*ANS(IS,N)*A2
              IF(IS-1,EQ,0)X1=0.5*X1
              A(IS)=X1
700 CONTINUE
            V1=-V1
            WRITE(IOUT,1001) (A(IS),IS=1,LP2)
            WRITE(LIB) A
600 CONTINUE
500 CONTINUE
900 CONTINUE
      ENDFILE LIB
      REWIND LIB
      PAUSE 999
1000 FORMAT(8F10,6)
1001 FORMAT(1H,12X,8F12.6,12X)
1100 FORMAT(1H1////////1H,36X,49HCONSTANTS TABLES TO TEXTURES CAL
  *CULATIONS)
2000 FORMAT(1H1////////1H,36X,48HTABLE OF LEGENDREA,S POLYNOMIALS
  *VALUES //)
2200 FORMAT(1H)
2500 FORMAT(1H1////////1H,27X,6HHKL = ,IS//)
3000 FORMAT(1H1////////1H,36X,48HTABLE OF CUBIC SYMETRICAL FUNCTI
  *ONS K //)
4000 FORMAT(1H1////////1H,43X,33HTABLE OF A,LNS COEFFICIENTS//)
5000 FORMAT(1H1////////1H,43X,34HTABLE OF B,LMIM COEFFICIENTS//)
6000 FORMAT(1H1////////1H,43X,34HTABLE OF A,LMNS COEFFICIENTS//)
END

```